Anat Embryol (2001) 204:59–80

ORIGINAL ARTICLE

M. Kálmán · R.M. Gould

GFAP-immunopositive structures in spiny dogfish, *Squalus acanthias*, and little skate, *Raia erinacea*, brains: differences have evolutionary implications

Accepted: 6 March 2001

Abstract GFAP expression patterns were compared between the brains of a spiny dogfish (*Squalus acanthias*) and a little skate (*Raia erinacea*). After anesthesia, the animals were perfused with paraformaldehyde. Serial vibratome sections were immunostained against GFAP using the avidin-biotin method. Spiny dogfish brain contained mainly uniformly-distributed, radially arranged ependymoglia. From GFAP distribution, the layered organization in both the telencephalon and the tectum were visible. In the cerebellum, the molecular and granular layers displayed conspicuously different glial structures; in the former a Bergmann glia-like population was found. No true astrocytes (i.e., stellate-shaped cells) were found. Radial glial endfeet lined all meningeal surfaces. Radial fibers also seemed to form endfeet and en passant contacts on the vessels. Plexuses of fine perivascular glial fibers also contributed to the perivascular glia. Compared with spiny dogfish brain, GFAP expression in the little skate brain was confined. Radial glia were limited to a few areas, e.g., segments of the ventricular surface of the telencephalon, and the midline of the diencephalon and mesencephalon. Scarce astrocytes occurred in every brain part, but only the optic chiasm, and the junction of the tegmentum and optic tectum contained large numbers of astrocytes. Astrocytes formed the meningeal glia limitans and the perivascular glia. No GFAP-immunopositive Bergmann glia-like structure was found. Astrocytes seen in the little skate were clearly different from the mammalian and avian ones; they had a different process system – extra large forms were frequently seen, and the meningeal and perivascular cells were spread along the surface instead of forming endfeet by processes. The differences between *Squalus* and *Raia* astroglia were much like those found between reptiles versus mammals and birds. It suggests independent and parallel glial evolutionary processes in amniotes and chondrichthyans, seemingly correlated with the thickening of the brain wall, and the growing complexity of the brain. There is no strict correlation, however, between the replacement of radial ependymoglia with astrocytes, and the local thickness of the brain wall.

Keywords Astrocytes · Ependymal cells · Brain evolution · GFAP · Glial cell evolution

M. Kálmán (✉)
Department of Anatomy, Histology and Embryology,
Semmelweis University, Tüzoltó 58, 1450 Budapest, Hungary
e-mail: kalman@ana1.sote.hu
Tel.: +36-1-2156920/3695, Fax: +36-1-2155158

R.M. Gould
New York State Institute
for Basic Research in Developmental Disabilities,
Staten Island, New York, USA

Introduction

The formation of a myelinated central nervous system required a divergent evolution of macroglial cells into oligodendroglia and astroglia. Astroglia from each gnathostome class are marked by glial fibrillary acidic protein (GFAP; Dahl and Bignami 1973; Onteniente et al. 1983; Dahl et al. 1985). Its presence in agnathans is controversial (Onteniente et al. 1983; Bignami et al. 1992; versus Wasowicz et al. 1994; Wicht et al. 1994). Chondrichthyans are phylogenetically close to the ancestors that developed a myelinated nervous system (Bullock et al. 1984; Wahneldt et al. 1986; Wahneldt 1990; Martin et al. 1992), and most divergent from other gnathastomes (Northcutt 1981; Butler and Hodos 1996). Whereas all other gnathostomes have an endothelial cell-based blood-brain barrier, chondrichthyes have a glial cell-based blood-brain barrier (Bundgaard and Cserr 1981, 1991; Gotow and Hashimoto 1984). Therefore it is important to include chondrichthyans in the comparative studies of glia.

Members of all major vertebrate radiations (agnathans, chondrichthyans, actinopterygians and sarcopterygians), have one of the two brain organizations: type I ("laminar") or type II ("elaborated"; Butler and Hodos 1996). In type I brains, neurons either remain in the periventricular zone or migrate only short distances

from it. In type II brains, neurons migrate extensively, and therefore these brains are larger and are composed of numerous nuclei. Based on this classification, batoids (rays and skates) and galeomorph sharks have type II brains, whereas squalomorph and squatinomorph sharks and chimeras have type I brains (Butler and Hodos 1996). Related to the body weight, the telencephalon is relatively small in these latter three groups, comparable to that of amphibians, whereas in batoids and galeomorph sharks the relative weight of the telencephalon is four to fifteen-fold greater (Northcutt 1981), and therefore comparable to that of birds and mammals. Batoids and galeomorph sharks have thick brain walls and narrow ventricles, whereas other chondrichthyans have thin-walled brains with wide ventricles. In batoids and galeomorph sharks numerous accessory sulci lend a foliated appearance to the cerebellum (Nieuwenhuys 1967). In these groups such cerebral connections exist that resemble those found in mammals, e.g. ascending thalamo-pallial pathways, but not in amphibians and teleost fishes (Northcutt 1981).

At the turn of the 19th and 20th centuries several papers investigated the glia of the cartilaginous fishes by impregnation methods (e.g., Houser 1901). Horstmann (1954) both reviewed the early work and carried it further. Immunostaining against GFAP, effective in all gnathostomes including chondrichthyans (*Squalus acanthias*: Dahl and Bignami 1973; Gould et al. 1995; *Mustelus canis*, *Raia ocellata*: Dahl et al. 1985), has allowed further comparisons. The previous immunohistochemical studies of GFAP in chondrichthyans, however, were confined to the demonstration of the cross-reactivity with mammalian anti-GFAP antibodies in vitro, and in some tissue samples, but did not map the distribution of the GFAP-immunopositivity systematically. It is to be noted that a recent study (Chiba 2000) detected another glial marker, S-100 in sharks (*Scyliorhinus torazame* and *Mustelus manazo*).

The present study demonstrates that the tendency of astroglial specialization in cartilaginous fishes is similar to that which has been found in amniotes (Onteniente et al. 1983; Linser 1985; Hajós and Kálmán 1989; Kálmán and Hajós 1989; Bodega et al. 1990; Monzon-Mayor et al. 1990; Yanez et al. 1990; Zilles et al. 1991; Kálmán et al. 1993; 1994; Kálmán 1998), i.e., astrocytes become predominant to ependymoglia, and the expression of GFAP regresses. Representative cartilaginous fishes with type I and type II brains, namely spiny dogfish (*Squalus acanthias*) and little skate (*Raia erinacea*), respectively, were used.

In this paper, the term “ependymoglia” refers to every glial element having perikarya in the ependyma. “Radial glia” refers to fibers that are oriented from the ventricle to the meningeal surface, independently of perikaryal position, while “radial ependymoglia” display both features. “Fibers” refers to GFAP-immunopositive glial fibers, unless otherwise specified. “Astrocyte” refers to stellate-shaped cells, whereas the term “astroglia” comprises astrocytes as well as the related glial structures, including ependymoglia and radial glia, in accordance with the terminology used by Mugnaini (1986).

Materials and methods

A young male spiny dogfish, *Squalus acanthias*, (25 inches long) and a male little skate, *Raia erinacea*, (18 inches long) were obtained at the Marine Biological Laboratory, Woods Hole, Mass. The animals were anaesthetised with 0.01% MS-222 (Sigma) in ice-cold seawater. When they became insensitive to handling, they were perfused through the exposed aorta with 4% paraformaldehyde in a 10% sucrose and 0.1 M phosphate buffer (pH 7.4). After perfusion the brains were removed and postfixed overnight in fresh fixative. Brains were rinsed in phosphate buffer (0.1 M, pH 7.4), embedded in agar, and 100-µm-thick serial sections were cut in the coronal plane with a vibration microtome (Vibratome). After overnight washing in phosphate buffer, the floating sections were pre-treated with 3% H_2O_2 (for 5 min) to suppress the endogenous peroxidase activity, and then incubated in 20% normal goat serum (for 1.5 h, at room temperature) to block the nonspecific antibody-binding. These and all subsequent steps included rinses with phosphate buffer between reagent changes. The primary antibody was mouse-monoclonal immunglobulin prepared against porcine GFAP (Boehringer, Mannheim), and applied at a 1:100 dilution (v:v; the final antibody concentration was 200 ng/ml) in phosphate buffer that contained 0.5% Triton X-100, for 60 h at

Fig. 1 Schematic drawings in cross-section of the *Squalus* telencephalon, in rostro-caudal order (**a** to **d**, **a** and **b** represent only one hemisphere). Note the large ventricle (*V*; *MP*, *LP* medial and lateral pallia, respectively; *S* septum; *TOl* origin of the olfactory tract). The ventricles fuse caudally (**d**), where the medial pallium forms an interhemispheric bridge. A dorsal recess (*lowercase v*, on the right side, which demonstrates a more caudal position) appears to be separated from the main (ventral) ventricle in cross sections. *Bar* 1 mm

Fig. 2 Enlarged part of *Squalus* telencephalic wall. Note the relatively even distribution of the radial fibers. These fibers start thick (*arrowhead*) at the ventricular surface (*V*), become thinner (*small double arrowhead*) toward the middle and then thicken into endfeet (*white asterisk*) at the meningeal surface (*M*). Their course is wavy, mainly near the surfaces. Four zones can be distinguished; *thick arrows* are oriented corresponding to the courses of the borders. Near the ventricle the radial fibers predominate, then a network of irregular fibers enmeshes them, then radial fibers become dominant again, and near the meningeal surface the fiber system seems to be denser due to the thickenings toward the endfeet. *Arrows* point to vessels with fine glial plexuses. *Bar* 60 µm

Fig. 3 In *Squalus*, glial fibers (*arrowheads*) follow an arching course where the thickness of the telencephalic wall is uneven, e.g., in the thickening of the medial pallium (*V* ventricular surface, *arrows* vessels – note the plexuses of fine glial fibers around them). *Bar* 60 µm

Fig. 4 Perivascular glia in the *Squalus* telencephalon. Thick radial fibers seem to form en passant contacts (*arrows*) or endfeet (*curved arrow*) on the blood vessels. Thin other glial fibers (*arrowheads*) form plexuses around the vessels. *Bar* 15 µm

Fig. 5 In the lateral pallium of *Squalus*, near the emergence of the olfactory tract, thin irregular fibers (*small double arrowheads*) predominate around the coarse fibers (*arrowheads*) and vessels (*arrows; curved arrow* points to an endfoot). *Bar* 60 µm

Fig. 6 *Squalus* septum. On each side, collaterally to the midline, a zone (*thick arrows*) has a relative paucity of fibers. Most fibers end at the border of this zone, only few penetrate to the vessels (*arrows*). *Bar* 60 µm

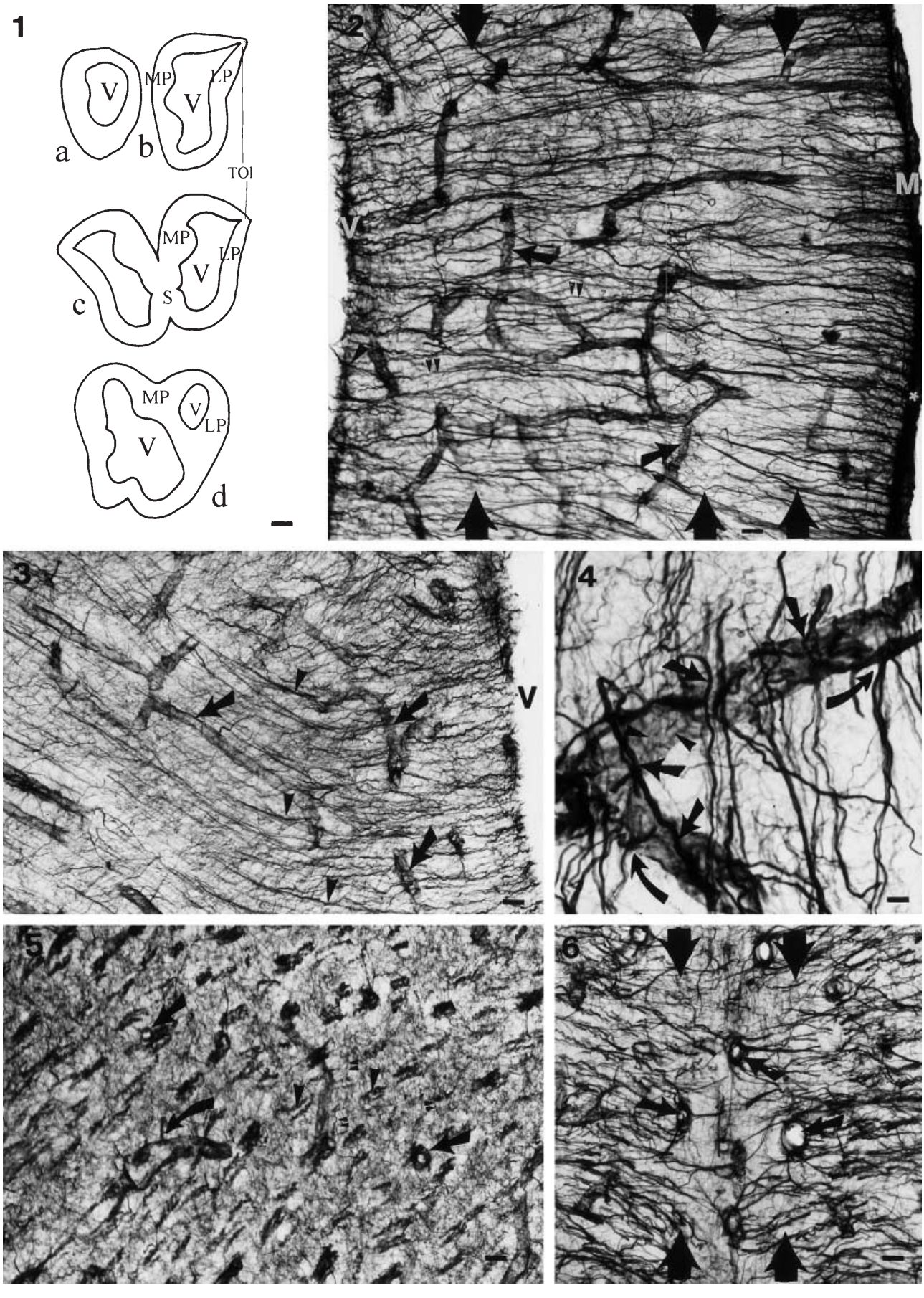
1
V
MP
LP
V
a
b
TOl
MP
LP
V
c
S
MP
V
LP
V
d
2
M
V
3
V
4
5
6

4°C. After that the sections were incubated with a secondary antibody, biotinylated rabbit anti-mouse immunoglobulin, then with streptavidin-biotinylated horseradish peroxidase complex, both reagent produced by Amersham, and applied at a dilution 1:100 in phosphate buffer, for 1.5 h at room temperature. The immunocomplex was visualized by incubation with 0.05% 3,3'-diaminobenzidine in 0.05 M TRIS-HCl buffer (pH 7.4) that contained 0.01% H_2O_2, for 10 min, at room temperature.

For orientation, every second section was stained with cresyl violet according to Nissl. With a microscope slide projector, a rostrocaudal series of drawings was made that showed the contours of the original sections of interest. All photomicrographs display GFAP-immunostained sections. The identification and nomenclature of brain structures are based on the descriptions of Ariens-Kappers et al. (1960), and Butler and Hodos (1996), and the atlas of Smeets et al. (1983). Additional related information can be found in Northcutt (1978) and Nieuwenhuys et al. (1997), especially for the telencephalon in Northcutt (1981), for the tectum in Schroeder and Ebbesson (1975), for the brain stem in Smeets and Nieuwenhuys (1976), and for the cerebellum in Nieuwenhuys (1967).

Results

Squalus acanthias: telencephalon

The spiny dogfish telencephalon comprises paired olfactory bulbs and evaginated hemispheres, and a caudal telencephalon medium. Structure of the telencephalon is illustrated in Fig. 1. The hemispheres contain large ventricles surrounded by a relatively thin brain wall, typical of type I brain structure. Caudally, the hemispheres fuse, have a common ventricle, and the dorsal and medial pallia form an interhemispheric bridge. The bridge appears as a slight bulge of the roof of the common ventricle. From the common ventricle dorsal recesses extend dorsocaudally, which appear as separate cavities in the sections of the most caudal part (see Fig. 1d, right side).

The GFAP immunoreactivity appears relatively even throughout the telencephalon. In the telencephalic wall the predominant GFAP immunostained elements are radial fibers that span the brain wall from the ventricle to the meningeal surface (Fig. 2). From the ventricular surface the fibers start thick, thin toward the middle and then thicken again and form endfeet on the meningeal surface. Their course is slightly wavering, mainly near the surfaces. According to the characteristics of the fibers, four zones can be distinguished. Near the ventricle the radial fibers predominate, then a network of irregular fibers enmeshes them, then radial fibers become dominant again, and near the meningeal surface the fiber system seems to be denser due to the thickenings toward the endfeet. The glial fibers follow an arched course where the thickness of the brain wall is uneven, e.g., in the bulky part of the medial pallium (Fig. 3). Radial fibers also seemed to form endfeet and en passant contacts on the vessels (Fig. 4). Plexuses of fine perivascular glial fibers also contributed to the perivascular glia. In the lateral pallium, near the emergence of the olfactory tract, thin irregular fibers predominate the full thickness of the wall (Fig. 5). Other than here, neither telencephalic areas nor nuclei are distinct with GFAP immunostaining. In the septum, in the fused walls of the hemispheres the radial fibers are oriented toward the midline. Most fibers do not cross the midline, but leave a zone of relative paucity of fibers collateral to the midline on each side (Fig. 6).

Squalus acanthias: diencephalon and mesencephalon

The diencephalon and mesencephalon are described together since in several sections both are present (see contours in Fig. 7). The optic chiasm (Figs. 8, 9) and tracts (Fig. 10) have relatively few GFAP-immunopositive fibers, which form septa between the optic fiber bundles. Most parts of the diencephalon contain a dense, almost

Fig. 7 Schematic drawing of cross-sections of the *Squalus* diencephalon and mesencephalic tectum, in rostro-caudal order (**a–d;** *ChO* optic chiasm, *CP* posterior commissure, *Hb* habenula, *Hy* hypothalamus; *LI* inferior lobe of hypothalamus, *RI* recess of the third ventricle in the inferior lobe of hypothalamus, *Th* thalamus, *TO* optic tract, *TeO* tectum, *3V* third ventricle – its roof, the lamina epithelialis, is missing; the site of its attachment is marked by *double arrow*, *VT* tectal ventricle, *asterisk* pineal recess, *arrow* central grey matter – see enlarged in Fig. 13). *Bar* 0.8 mm ▶

Fig. 8 Cross-section of the *Squalus* diencephalon at the level of the optic chiasm (*ChO*), corresponding to the drawing in Fig. 7a. The chiasm has relatively little GFAP immunopositivity, which is represented by glial septa (*arrowheads*) between the optic fiber bundles (see enlarged in Fig. 9, lower middle part of the panel). Other regions are colonized by dense and thin glial fibers (*small double arrowheads*). The roof of the third ventricle (3 V) is missing (*M* meningeal surface). *Bar* 300 µm

Fig. 9 Enlarged detail of the optic chiasm. *Arrowheads* point to the glial septa between the bundles of optic fibers. *Bar* 60 µm

Fig. 10 Cross-section of the *Squalus* diencephalon, between Figs. 7b and 7c. In the optic tract (*TO*) the only GFAP-immunopositive elements are glial septa (*arrowheads*) between the optic fiber bundles. Other regions (*Hb* habenula, *Th* thalamus, *Hy* hypothalamus) are colonized by thin fibers, which are less densely packed around the inferior recess (*RI*) of the third ventricle (*3V*) in the inferior lobe of the hypothalamus. The bottom and the roof of the third ventricle (*3V*) are missing, the attaching place of the roof (lamina epithelialis) is pointed by *double arrow* (*M* meningeal surface). *Bar* 300 µm

Fig. 11 Enlarged part of the wall of the inferior recess in the inferior lobe of the hypothalalmus (*M, V* meningeal and ventricular surfaces, respectively). The fibers are thin (*arrowheads*) near the ventricle, course in a radial direction, and form thick meningeal endfeet (*curved arrows*). *Arrows* point to vessels with plexuses of fine glial fibers. *Bar* 60 µm

Fig. 12 The posterior commissure (*CP*) of *Squalus*, and the surrounding areas. The middle part of the commissure is not in the plane of section, which is behind Fig. 7d. The area of the tracts that collect into the commissure is light, poor in GFAP-immunopositive structures, which are mainly coarse septa (*arrowheads*) between the nerve fiber bundles. Other regions are rich in GFAP-immunopositive fibers, especially the central grey (*G; 3V* third ventricle, *VT* tectal ventricle). *Bar* 300 µm

Fig. 13 Enlarged detail of diencephalic central grey (*G*). *Arrowheads* mark radial fibers emerging from the grey matter, *curved arrow* points to light spots corresponding bundles of nerve fibers. *Bar* 60 µm

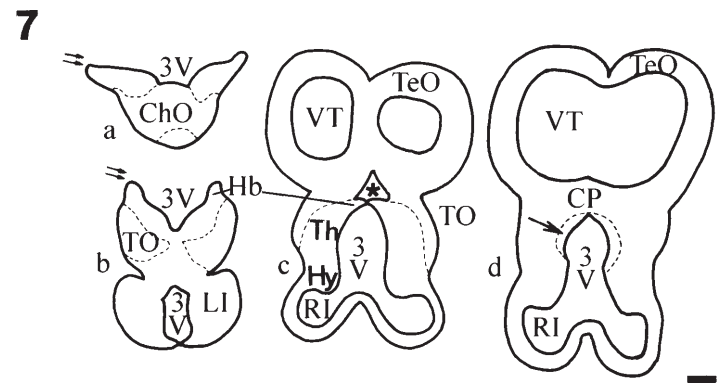
7
3V
ChO
a
VT
TeO
3V
Hb
TO
b
Th
3
V
c
Hy
RI
LI
3
V
TeO
VT
CP
d
3
V
RI

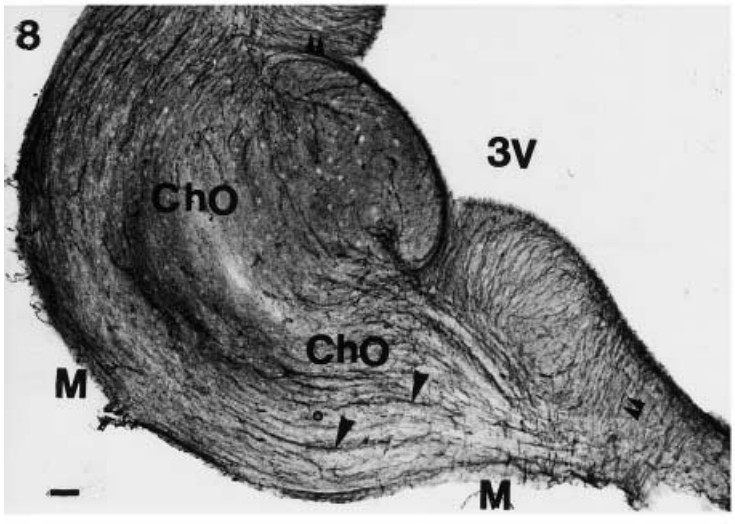
8
3V
ChO
ChO
M
M

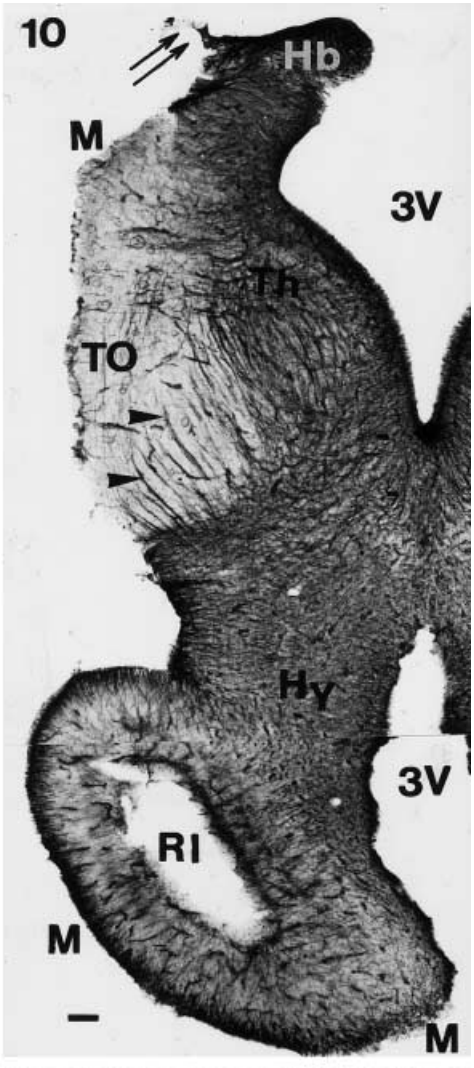
10
Hb
M
3V
Th
TO
Hy
3V
RI
M
M

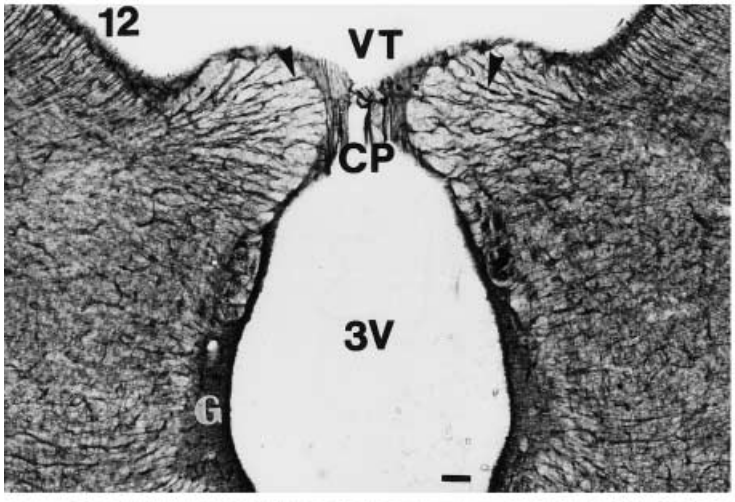
12
VT
CP
3V
G


M
V
11

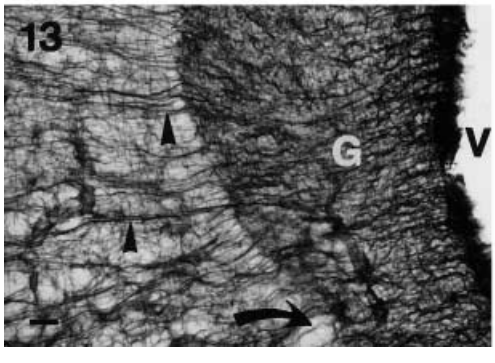
13
G
V


9
V

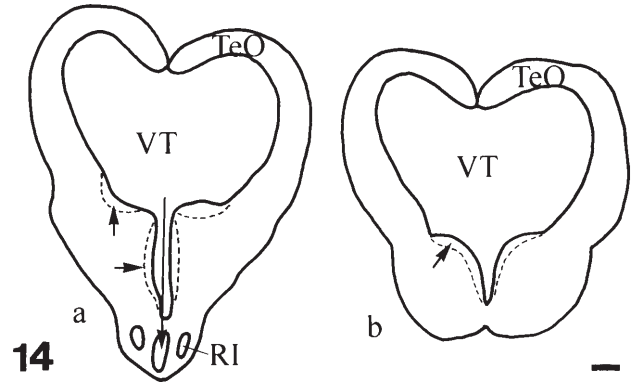

Fig. 14 Schematic drawings of *Squalus* diencephalon and mesencephalon in cross section, arranged in rostro-caudal order (**a**–**b**), continuous with drawings in Fig. 7 (*RI* inferior recess of the third ventricle, *TeO* optic tectum, *VT* tectal ventricle, *short arrows* central grey matter, *long arrow* points to the infundibulum). *Bar* 0.8 mm

Fig. 15 Enlarged part of the *Squalus* optic tectum. GFAP immunopositivity is quite evenly distributed with only slightly alterations in each tectal layer. The stratum superficiale (*SF*) contains only radial fibers forming endfeet on the meningeal surface (*M*). In the stratum album centrale (*CA*) there are bundles of myelinated nerve fibers (light spots indicated by *curved arrows*), whereas stratum griseum centrale (*CG*) contains only a dense system of radial fibers (*small arrowheads*) and other glial fibers. The periventricular layer (*PV*) has bundles of ependymal fibers which frequently surround vessels (*double arrowheads; VT* tectal ventricle). *Bar* 60 µm

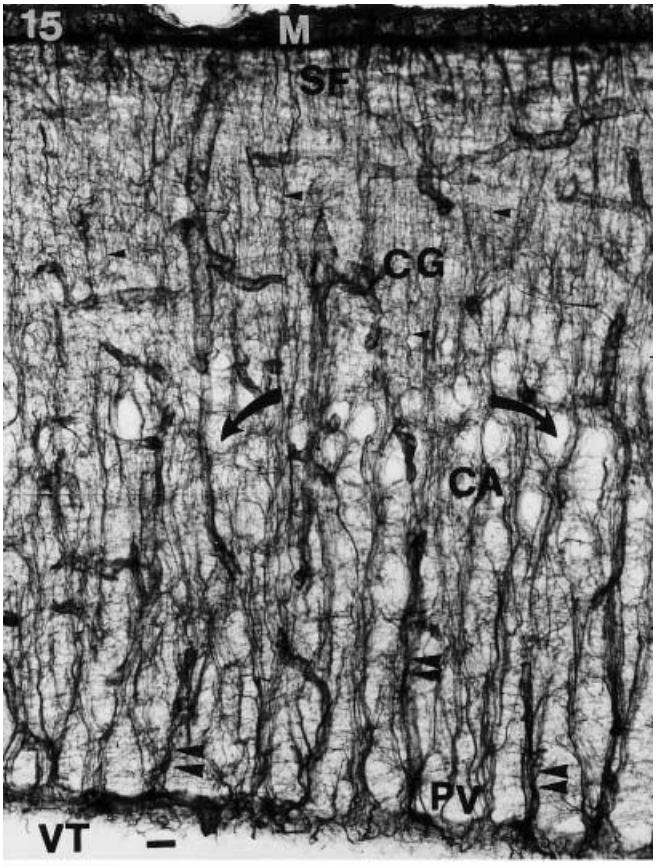

Fig. 16 Enlarged part of the *Squalus* mesencephalic tegmentum, between Figs. 14a and 14b. Radial fibers predominate. A denser fiber network marks the central grey (*G*), while light spots (*curved arrows*) correspond to bundles of nerve fibers (*VT* tectal ventricle). *Bar* 60 µm

Fig. 17 Schematic drawings of the cross-sections of the *Squalus* rhombencephalon, in caudo-rostral order (**a**–**e**). The right sides of the drawings represent more rostral situations (*arrows* grey matter, *single arrowheads* the molecular layer of cerebellar crest, *Cr*, later that of auricules, superior and inferior, *AS* and *AI* respectively, *g* the grey matter of cerebellar crest, *R* area of reticulated glial composition – see Fig. 20, *4V* fourth ventricle, its roof is missing, *double arrowheads* midline glial deptum, *double arrow* emergence of a cranial nerve). *Bar* 1 mm ▶

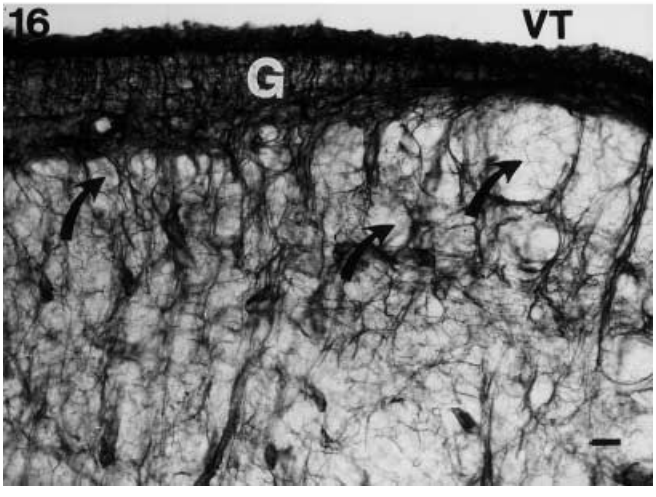

Fig. 18 Detail of the spinal cord of *Squalus*, the dorsal side is to left. The grey matter (*G*) has a dense fiber system. The nerve fiber bundles of the white matter (*W*) are separated by glial fiber bundles (*arrowheads; C* central canal, *FLM* medial longitudinal fasciculus). *Bar* 50 µm

Fig. 19 The "closed" part of the *Squalus* rhombencephalon, caudal to Fig. 17a. Three territories are distinguished: (1) grey matter (*G*) contains fine, dense, less regular fibers; (2) white matter (*W*) has large GFAP-free fields of nerve fibers, interspersed with glial fiber bundles; (3) a reticulated glial composition (*R* see enlarged in the next figure), which consists of thick bundles of glial fibers surrounding small light, GFAP-free spots. Its position approximately corresponds to that of the formatio reticularis (*C* central canal, *FLM* medial longitudinal fascicle, *double arrowheads* dorsal and ventral glial septa). *Bar* 300 µm

Fig. 20 Detail of the reticulated glial composition seen in the previous figure. Thick bundles of glial fibers surround small light, GFAP-free areas (*C* central canal, *G* grey matter, *double arrowhead* dorsal glial septum). *Bar* 60 µm

Fig. 21 Medial zone of the "open" part of the *Squalus* rhombencephalon. This region consists of neural tracts (*FLM* medial longitudinal fascicle), which are divided into bundles by glial septa (*arrowheads*). In the midline a thick population of fine, evenly distributed fibers forms a median septum (*Sm*), which widens fan-shaped toward the meningeal surface (*M*). The confined grey matter (*G*) contains densely packed fibers (*arrows* point to vessels, *4V* fourth ventricle). *Bar* 150 µm

Fig. 22 Intermediate zone of the "open" part of the *Squalus* rhombencephalon. Its structure mainly reflects the reticulated glial composition (*R*) seen in Fig. 20. The glial structures of grey matter (*G*; *LX* vagal lobe, see lateral arrows in Figs. 17b, c) and white matter (*W*) are confined near the fourth ventricle, *4V*, and the meningeal surface, *M*, respectively. *Bar* 150 µm

Fig. 23 The lateral zone of the "open" part of the *Squalus* rhombencephalon with a portion of cerebellar crest (*Cr; G* grey matter, *g* the grey matter of cerebellar crest, *m* the molecular layer of cerebellar crest, *M* meningeal surface, *R* reticulated glial composition, *4V* fourth ventricle, *W* glial pattern of white matter, near the emergence of a cranial nerve, see double arrow in Fig. 17c). *Bar* 300 µm

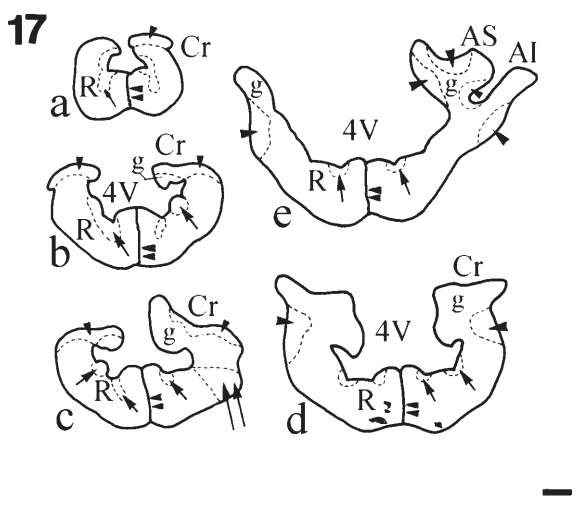
17
a
Cr
R
b
Cr
g
4V
R
c
Cr
g
R
d
Cr
g
4V
R
e
AS
AI
g
g
4V
R

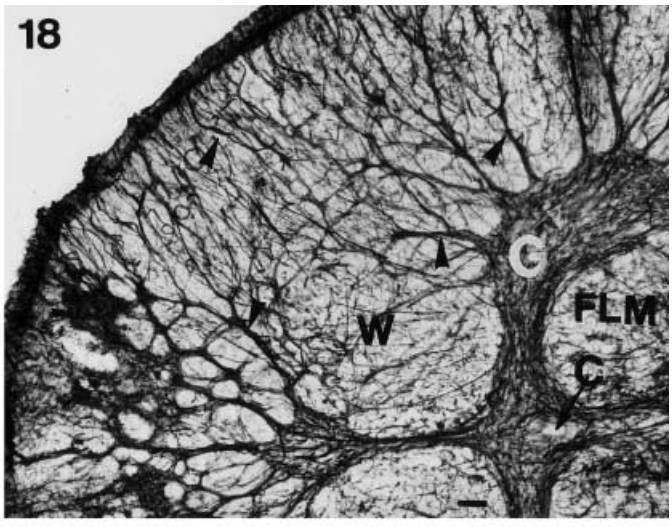
18
C
W
FLM
C

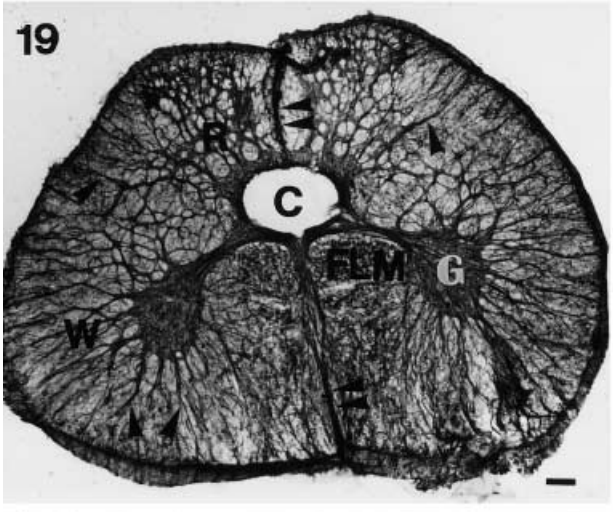
19
R
C
FLM
G
W

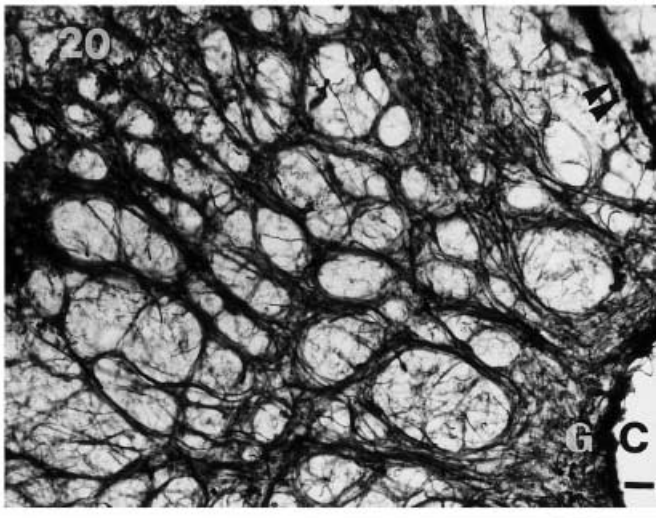
20
G
C

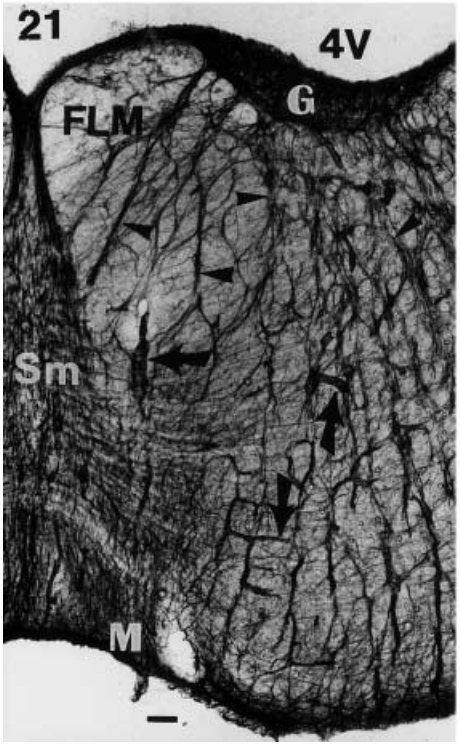
21
4V
G
FLM
Sm
M

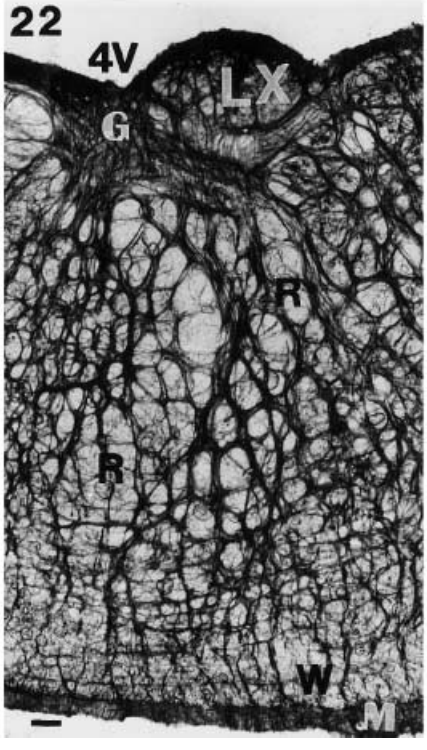
22
4V
G
LX
R
R
W
M

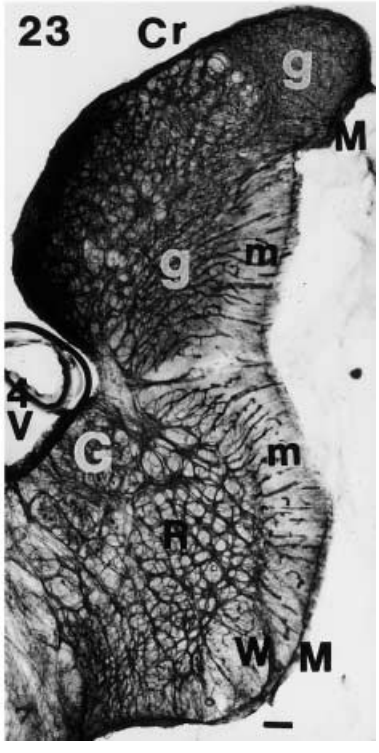
23
Cr
g
M
g
m
4
V
C
m
R
W
M

obscure system of fine glial fibers, the highest amounts running between the ventricular and meningeal surfaces. The glial fibers are less densely packed around the inferior recess of the third ventricle, in the inferior lobe of the hypothalamus (Figs. 10, 11). These fibers start thin at the ventricle, course in a radial direction, in general, and form thick meningeal endfeet. Nerve tracts that collect in the posterior commissure have relatively few GFAP-immunopositive glial fibers (Fig. 12), which separate the nerve fiber bundles. The other parts were rich in GFAP-immunopositive fibers, especially the central grey (Fig. 13). The radial fibers are almost obscured by the fine irregular fibers; they are conspicuous only where emerging from the central grey.

The *Squalus* tectum is formed by thin-walled domes that overlie the large tectal ventricle (Fig. 14). Radial fibers are the main GFAP-immunopositive elements, they are quite uniformly distributed, even with slight differences in each tectal layer (Fig. 15). The tectum has four layers: stratum periventriculare (or cellulare internum), stratum album centrale (or medullare internum), stratum griseum centrale (or cellulare externum) and stratum superficiale (or medullare externum) (Ariens-Kappers et al. 1960; Schroeder and Ebbesson 1975; Butler and Hodos 1996). The superficial layer contains fine, evenly distributed radial fibers forming endfeet on the meningeal surface. In the stratum album centrale myelinated nerve fiber bundles appear as light spots. The stratum griseum centrale lacks these spots and is filled with a dense network of fine fibers. The periventricular layer contains ependymal fiber bundles, frequently grouped around perpendicularly oriented vessels.

In the mesencephalic tegmentum, radial fibers also predominate. A dense fiber network marks the central grey (Fig. 16), with light areas corresponding to myelinated nerve fiber bundles including the medial longitudinal fascicle.

Squalus acanthias: spinal cord and rhombencephalon

Here the description begins at the spinal cord and continues rostralward. The contours of the rhombencephalon are illustrated in Fig. 17, with a part of the cerebellum, the cerebellar crest. This latter structure (crista cerebelli, lobus lineae lateralis anterior, see Nieuwenhuys 1967; Butler and Hodos 1996) is found only in fishes, and is integrated with the brain stem as it forms the rim of the rhombencephalic fossa. The contours of the cerebellar crest become complex rostralward, where it continues into the auricles of cerebellum (Fig. 17e; see also next subsection).

In the spinal cord (Fig. 18) the grey-matter astroglia consist of a dense meshwork of fine glial fibers, whereas the white matter contains glial fiber bundles that emanate from the grey matter toward the meningeal surface. Unstained regions represent myelinated nerve-fiber bundles.

The closed posterior part of the rhombencephalon (Fig. 19) resembles the spinal cord, except it has a wider central canal. A transitional area appears, however, between the grey and white matters. In this area loose yet thick bundles of glial fibers surround relatively small light, GFAP-free spots that likely represent myelinated nerve fiber bundles (Fig. 20) Therefore, a “reticulated” glial composition is formed, which shares characteristics of both grey and white matter, alternatively. Its position approximately corresponds to that of the formatio reticularis. Otherwise, the glial staining patterns of grey and white matters were similar to the spinal cord.

In the anterior, “open” part of the rhombencephalon, in the medial zone the medial longitudinal fascicle contains only a few dispersed GFAP-immunopositive glial fiber bundles, generally oriented toward the basal surface (Fig. 21). The confined grey matter contains a fine, dense, almost obscure fiber system. A fine evenly-distributed fiber population of the median glial septum widens to a fan-shaped structure ventrally. More lateral, in the intermediate zone of the section, the aforementioned “reticulated” glial composition predominates (Fig. 22).

Fig. 24 Enlarged detail of the cerebellar crest of *Squalus*. The glial pattern distinguishes the molecular layer (*m*) from the grey matter (*g*). *Arrows* point to vessels, note the plexus of fine glial fibers around them (*M* meningeal surface). *Bar* 60 µm ▶

Fig. 25 Schematic drawings of cross-sections of the *Squalus* cerebellum (**a**–**d**), and their positions in a sagittal section **e**. **Fig. 25a** is rostral to Fig. 17e. The cerebellar corpus extends over both the mesencephalon and the rhombencephalon, and has a similar structure in both directions (*ChO* optic chiasm, *EM* median eminence, *VC* cerebellar ventricle – note its recesses pointed in Fig. 25a, *VT* tectal ventricle, *4V* fourth ventricle. The dotted line in the longitudinal section show the position of the missing roof, the lamina epithelialis, of the ventricle. *Arrowheads* mark the molecular layer, *g* granular layer (granular eminence), *small arrow* (in **a**, **e)** points to the so-called “lower lip”, and the eminentia ventralis. *Double arrowhead* indicates the medial longitudinal fasciculus, *double arrow* points to the dorsal glial septum in the cerebellum. In Fig. 25b *asterisk* and *double asterisk* mark the positions of Figs. 26 and 28, respectively). *Bar* 1 mm

Fig. 26 Cerebellum of *Squalus*. The anatomical position is marked with *asterisk* in Fig. 25b. The relationship betweeen the granular layer (granular eminence, *g*) and the molecular layer (*m*) is conspicuous (*M* meningeal surface, *P* zone of Purkinje cells, *VC* cerebellar ventricle, *double arrow* points to the dorsal glial septum, *arrows* point to the vessels pointed also in Fig. 27 or 29). *Bar* 120 µm

Fig. 27 Detail of the granular eminence. Note the thick plexus of glial fibers. *Arrows* point to the same vessels as in Fig. 26 (*VC* cerebellar ventricle). *Bar* 60 µm

Fig. 28 Detail of the molecular layer (*m*) where it is not adjacent to the granular eminence. The anatomical position is marked with *double asterisk* in Fig. 25b. Note the fine fibers (*double arrowheads*) in the molecular layer. These fibers originate from the Purkinje cell layer (*P*) and are oriented toward the meningeal surface (*M*), like Bergmann glia. Coarse glial fiber bundles (*arrowheads*) separate the nests of Purkinje cells (*VC* cerebellar ventricle, *arrow* points to a vessel). *Bar* 60 µm

Fig. 29 Detail of the molecular layer (*m*), where it is adjacent to the granular eminence. Note the fine fibers (*small double arrowheads*) like Bergmann glia in the molecular layer. At this segment of the molecular layer transverse fibers are also seen (*curved arrows; M* meningeal surface, *P* Purkinje cells; *arrow* points to the same vessel as in Fig. 26). *Bar* 60 µm

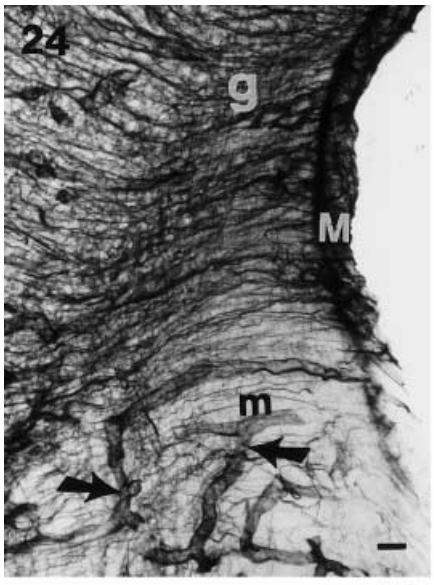
24
g
M
m

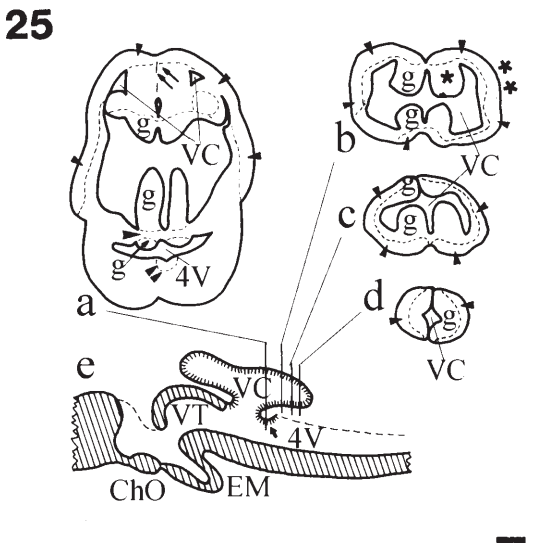
25
g
VC
g
4V
a
b
g
g
VC
c
g
g
d
g
VC
e
VC
VT
4V
ChO
EM


26
M
m
P
g
g
VC

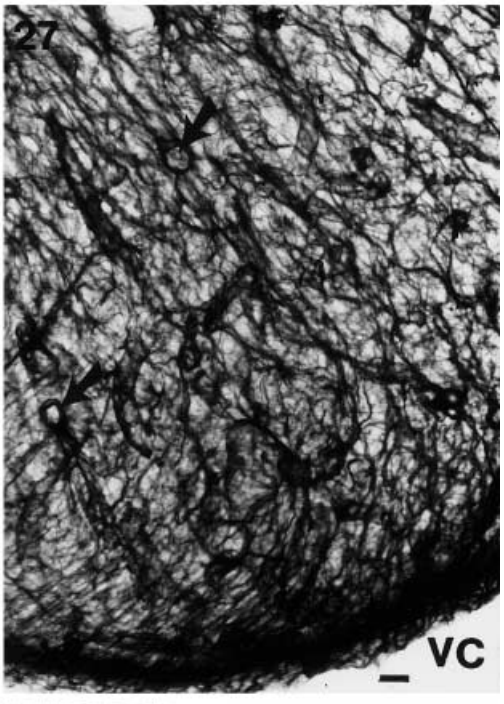
27
VC

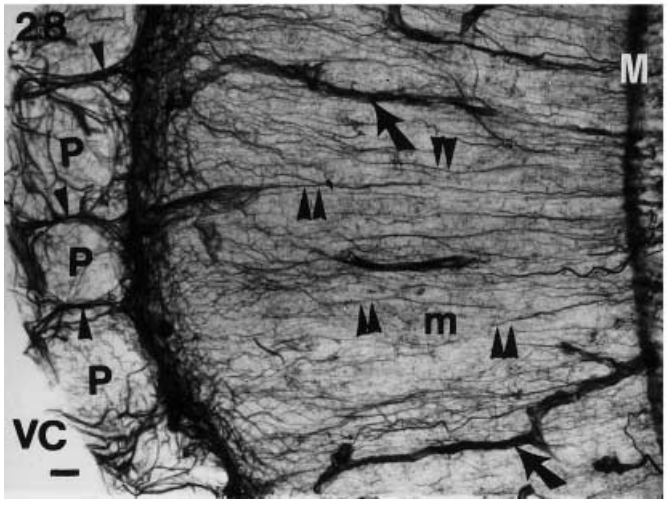
28
M
P
P
P
m
VC

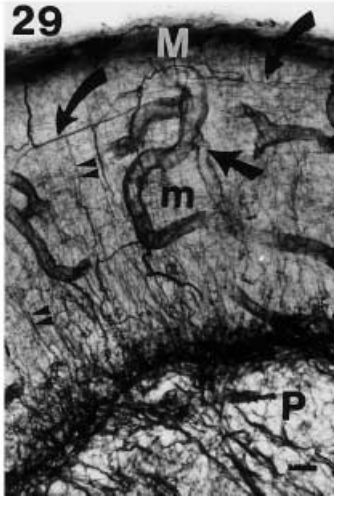
29
M
m
P

The glial structures of the grey and white matters are confined near the ventricular and meningeal surfaces, respectively. The lateral zone of the sections continues into the aforementioned cerebellar crest. The glial patterns (Fig. 23) of the grey matter, the "reticulated" glial composition, and the white matter (at the emergence of cranial nerves) are similar to the more medial regions. In the cerebellar crest (Fig. 24) the grey matter also contains a dense, obscure fiber system, and a molecular layer like in the cerebellum is distinguished by less densely packed fibers perpendicular to the surface.

Squalus acanthias: cerebellum

The structure of the cerebellum is demonstrated in the drawings of Fig. 25 (after Nieuwenhuys 1967). The large, complex oval-shaped cerebellar corpus overlies the medulla and the midbrain. The rostral and caudal ends of the corpus, therefore, seem to be separate in cross-section from the mesencephalon and the rhombencephalon, respectively. The cerebellar corpus encloses a large cerebellar ventricle, which is confluent with the fourth ventricle. Around the cerebellar ventricle, four walls can be distinguished. The caudal wall ends in a so-called "lower lip", a band of nervous tissue above the fourth ventricle. Due to the turning of the caudal cerebellar wall, the "lower lip" is separated from the cerebellar corpus by a deep groove. The rostral wall is continuous with the tectum as well as the lateral walls with the pons. Inside the ventricle, there are paired columns, the granular eminences. They run adjacent to the cerebellar midline, on both the roof of the ventricle and its floor, where they turn caudally on the lower lip as a paired eminentia ventralis. Here they are continuous with the upper leaves of the auricules (see also Fig. 17e), while these latter reflex into the lower leaves, and therefore finally the granular eminences are continuous with the grey matter of cerebellar crest described in the previous subsection.

The granular eminences overlap only the medial portions of the molecular layer. Their glial structures are easy to distinguish by GFAP immunostaining (Fig. 26). The granular eminence contains a thick plexus of irregularly coursing fibers (see also Fig. 27), whereas the molecular layer contains a dorsal glial septum in the midline, and fine fibers that are perpendicular to the meningeal surface and originate in the zone of Purkinje cells (Fig. 28). These fibers resemble Bergmann glia. Thick fiber bundles outline nests for the Purkinje cells. Where the molecular layer is adjacent to the granular eminence (Fig. 29), transverse fibers are also present.

Raia erinacea: telencephalon

The contours of the rostral part of the *Raia* telencephalon are illustrated in Fig. 30. Compared with spiny dogfish, little skate telencephalic ventricles are small and extremely narrow, and are not found in the most rostral brain sections. The hemispheres fused with each other in their full length. The skate telencephalon has comparatively few GFAP-immunopositive elements, which are unevenly distributed. The GFAP immunoreactivity is confined to periventricular, perivascular and submeningeal glia (Figs. 31, 32), and the latter two are mainly astrocytic in nature. More astrocytes have been found in the medial part of the telencephalon, which is demarcated by sagittal planes through the ventricles (i.e., the septum and the medial pallium), than in the lateral pallium. In the medial part two systems of vessels can be distinguished. One contains thin vessels and located dorsally, in the medial pallium, the other one consists of thick vessels at the midline, rostroventrally, in the septum.

The perivascular glia in the telencephalon is composed from single short fibers and astrocytes (Figs. 32, 33), but the perikarya-like empty circles on the vessels suggest that the fibers originate from the vessels and do not end on them (Fig. 33). Note that larger vessels have a denser perivascular glia than smaller vessels.

The meningeal surface of the *Raia* telencephalon is colonized with astrocytes (Fig. 34). These cells are spread along the surface like starfish on the bottom of the sea. The GFAP-free places of nuclei are easily seen.

Fig. 30 Schematic drawings of the cross-sections of the anterior portion of the *Raia* telencephalon, in rostro-caudal order (**a–c**). Note the narrow ventricles (*V*), which do not extend into the rostral part (Fig. 30a) of the telencephalon. Dotted contours within the telencephalon surround the GFAP-rich areas that are mainly around the vessels and the ventricle. Note these areas are absent in the rostral part (Fig. 30a). (*MP, LP* medial and lateral pallia, respectively, *S* septum, *TOl* olfactory tract). *Bar* 1 mm ▶

Fig. 31 The medial part of the *Raia* telencephalon (corresponding to Fig. 30c). The GFAP immunopositivity is confined to the perivascular glia (*double arrowheads*, see a similar area enlarged in the Fig. 32), submeningeal glia (*arrowheads*, see a similar area enlarged in Fig. 34) and periventricular glia (*curved arrows; V* ventricle, see a similar area enlarged in Fig. 35). Note the heavy labeled perivascular glia of the vessels (*large double arrowheads*) in the midline (*S* septum) and the dense system of thin vessels in the medial pallium (*MP*). *Bar* 300 µm

Fig. 32 Submeningeal and perivascular glia in the medial pallium (*MP*), similar to that seen in Fig. 31. Note the endpieces of perpendicular fibers (*arrowheads*) below the meningeal surface. *Double arrowheads* point to vessels. *Bar* 150 µm

Fig. 33 Perivascular glia in the *Raia* telencephalon, enlarged from the right upper corner of Fig. 32. Stellate-shaped cells and single fibers are visible. The fibers originate from perikarya-like clear circles (*arrows*) on the vessels. Note that larger vessels have denser perivascular glia than the smaller ones. *Arrowhead* points to the endpiece of a fiber perpendicular to the meningeal surface. *Bar* 60 µm

Fig. 34 The meningeal surface is lined by astrocytes which are spread along it in *Raia*. *Arrows* point to the GFAP-free places of nuclei, arrowheads point to the endpieces of fibers perpendicular to the meningeal surface. Because the figure represents the ventrolateral surface of the lateral pallium (*LP*), it is not particularly rich in vessels. *Bar* 60 µm

Fig. 35 Ventricle (*V*) and associated radial fibers (*curved arrows*) in *Raia* telencephalon, similar to that seen in Fig. 31. The radial glia seem to be confined to an area near the ventricles, the fibers cannot be traced to the meningeal surface. *Bar* 150 µm

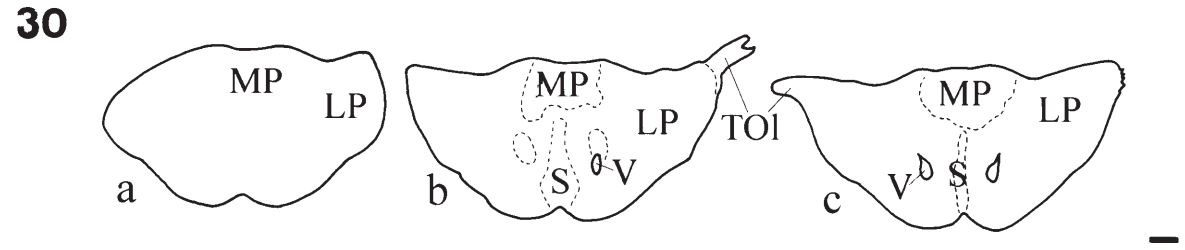
30
MP
LP
a
MP
LP
TOl
S
V
b
MP
LP
V
S
c

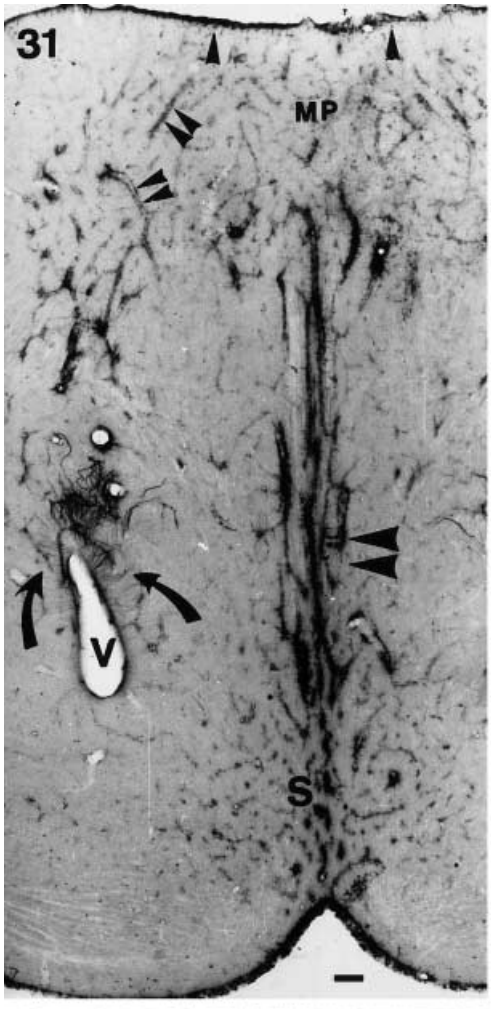
31
MP
V
S

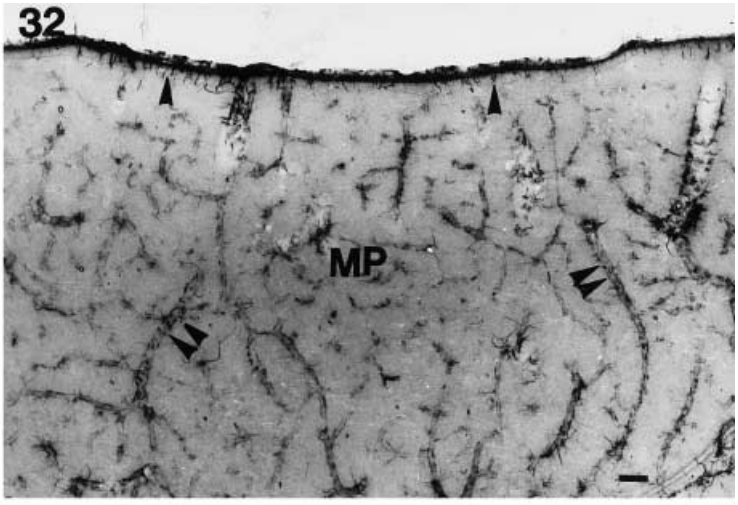
32
MP

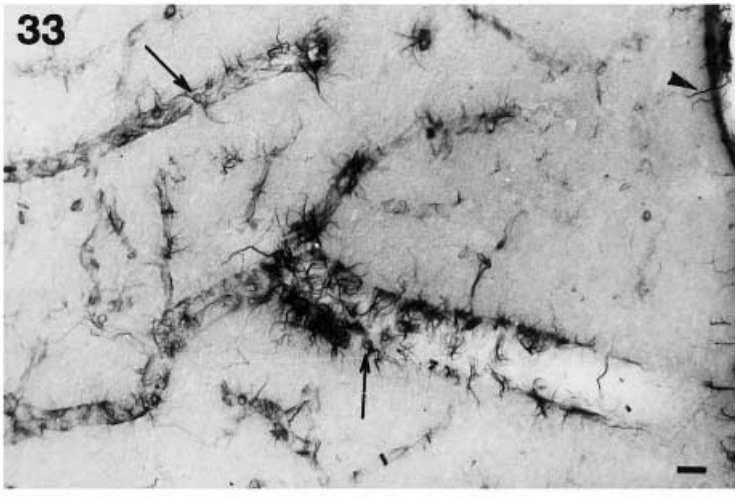
33

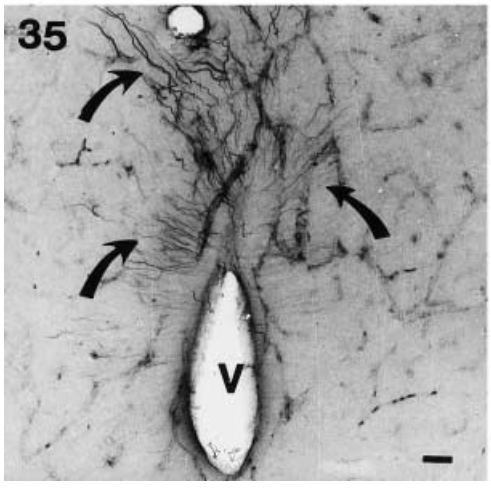
35
V

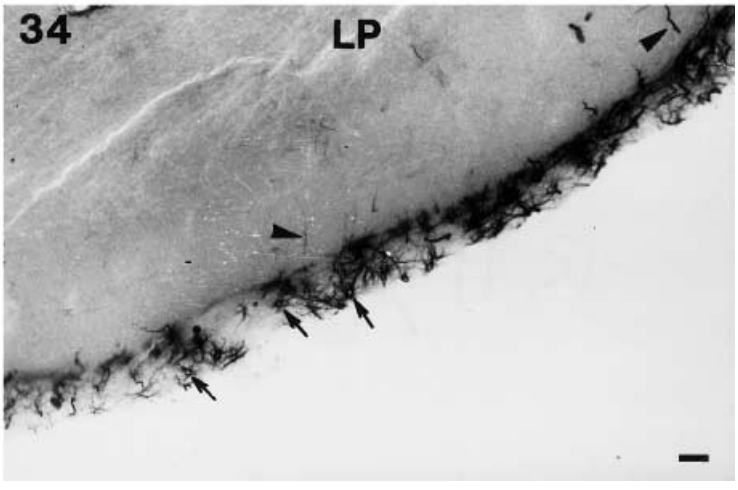
34
LP

Single fibers are also found, which run perpendicular to the meningeal surface, in greater number along the dorsal surface (Fig. 32). The perikarya that belong to them are not apparent.

Dense systems of radial glia are confined to regions just above the ventricles (Fig. 35). They orient toward the dorsal surface, but cannot be followed there.

In the olfactory tract (Fig. 36) glia form long fibers, which course longitudinally in parallel with the nerve fibers, and not perpendicular to the meningeal surface, as it would be expected for radial glia. These fibers did not penetrate the pallium.

Proceding caudalward from the olfactory tract toward the optic chiasm the ventricles join to form a single cavity (Fig. 37), and two dorsal recesses extend from them. In this posterior part of the telencephalon the types of GFAP-immunopositive elements (Fig. 38) are similar to those seen previously, except for the regions where the dorsal recesses of the ventricular system come near the meningeal surface (Fig. 39). Here alone, radial fibers could be followed to the meningeal surface. In contrary, where the ventricles join ventrally, only weak ventral and dorsal midline glial septa represent the radial glia (Fig. 40). In the lateral pallium high-power view reveals fine scattered fibers (Fig. 41), which point toward the meningeal surface.

Raia erinacea: diencephalon and mesencephalon

Contours of the diencephalon and mesencephalon, which are found together in several sections, are illustrated in Fig. 42. The shape of the *Raia* optic tectum is quite different from that of *Squalus*, although they share the same cytoarchitectonic layers (Ariens-Kappers et al. 1960; Butler and Hodos 1996). The *Raia* mesencephalic ventricle, however, is relatively narrow and triangular, and the tectal wall is thick.

Few GFAP immunoreactive elements are found in the diencephalon and mesencephalon (for general views, see Figs. 43, 44). The astrocytes, however, although scarce, are so large that it is easy to find them even under low-power objective (see also Fig. 42). The anterior part of the diencephalon (Fig. 43) contains a prominent fan-shaped radial fiber system with its apex pointed toward the ventricle. This fiber system, which is dense in the middle, but less dense laterally, penetrates the optic chiasm, too. The most lateral region of the diencephalon contains astrocytes but no long fibers. The lobus inferior of the diencephalon is relatively large, with an inferior recess of the third ventricle, which is surrounded by GFAP-immunopositive ependymal cells (Fig. 44, inset in the right lower corner). Ependymal cells do not express GFAP immunopositivity anywhere else in the ventricular system. In both the diencephalon and mesencephalon the meningeal surface is lined with astrocytes (Figs. 45, 46) similar to that of the telencephalon.

The optic nerve is penetrated by dense GFAP-immunopositive perpendicular fibers, with intermingled astrocytes (Fig. 47). In contrast, in the optic tract only a few but large astrocytes are visible, as well as a few glial fibers oriented along the nerve fibers (Fig. 48). The posterior commissure contains astrocytes as well as perpendicular and horizontal glial fibers, the latter ones running along the nerve fibers (Fig. 49).

Radial glia are present in the diencephalon, and to a lesser extent in the mesencephalon. The radial glial system that predominates in the middle of the diencephalon, is intermingled with astrocytes (Figs. 43, 50). In the midbrain tegmentum even at high-power very few long fibers appear, which are oriented to the meningeal surface (Fig. 51). Otherwise the radial fiber system is confined to the midline in the mesencephalon, as the dorsal and ventral glial septa (Figs. 52, 53). The fibers clearly run from the ventricle to the meningeal surface. Long glial fibers form endfeet in the medial side of the optic tectum, immediately above the posterior commissure (Fig. 54). Their origin could not be traced.

In both the diencephalon and mesencephalon large astrocytes are found scattered, mainly below the meningeal surface, and to a lesser extent near the ventricle (see scattered dots in Fig. 42). A more dense population is located at the juncture of the tegmentum and optic tectum (Figs. 44, 55). Typical astrocytes are seen enlarged in Figs. 55 to 59. These astrocytes lie far from vessels and are unusually large compared with the perivascular astrocytes in the mesencephalon (Fig. 51) and telencephalon (Fig. 33). They are also much larger than typical mammalian or avian astrocytes. Their arborization appears to consist of two to four thick main branches, each spreading to fine secondary branches. Intermediate

Fig. 36 Longitudinally arranged glial fibers in the olfactory tract (*TOl*) of *Raia*. Note the abrupt disappearance of staining at the origin of the tract (to right). *Bar* 100 μm ▶

Fig. 37 Schematic drawings of the cross-sections of the posterior *Raia* telencephalon, in rostro-caudal order (**a–c**). Caudalward the ventricles (*V*) fuse ventrally (*lower pointer*), but extend dorsal recesses (*upper pointer*). Dotted contours inside the telencephalon surround the GFAP-rich areas around the vessels and ventricles. Note they are absent in the most caudal part (**c***; ChO* optic chiasm, *MP, LP* medial and lateral pallia, respectively, *S* septum, *small arrows* dorsal and ventral midline glial septa). *Bar* 1 mm

Fig. 38 The medial pallium (*MP*), corresponding to Fig. 37b. The arrangement of the GFAP-immunopositive elements is similar to that shown in Fig. 31 (note the identical marks: *arrowheads* submeningeal glia, *double arrowheads* perivascular glia, *curved arrows* periventricular radial glia). The ventricles (*V*) are going to fuse ventrally, but extend dorsal recesses (*v*). *Bar* 200 μm

Fig. 39 Dorsal recess (*v*) of the *Raia* ventricular system located near the meningeal surface (see also in Fig. 37c). Radial fibers (*curved arrows*) can be followed to the surface. *MP, LP* medial and lateral pallia, respectively. *Bar* 200 μm

Fig. 40 The fused part of the ventricular system (*V*) in *Raia*, between Figs. 37b and 37c. Only faintly stained ventral and dorsal midline glial septa represent the radial glia (*arrows*). *Bar* 200 μm

Fig. 41 Fine fibers (*arrowheads*) in the lateral pallium of *Raia*, oriented toward the meningeal surface. *Double arrowheads* point to vessels with perivascular astrocytes. *Bar* 60 μm

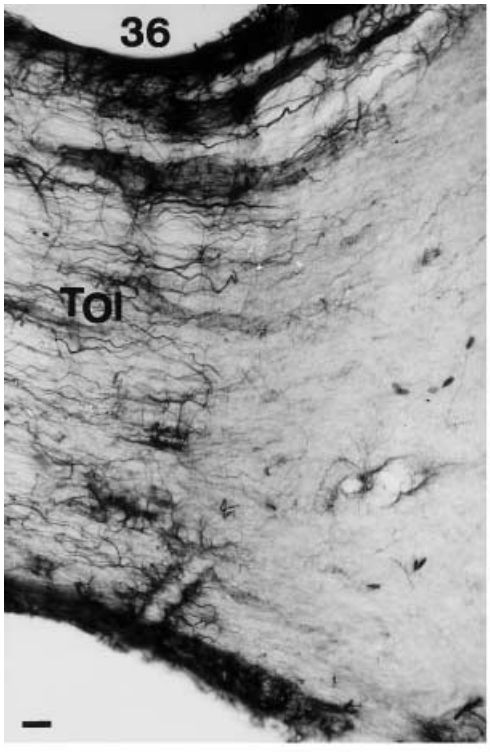
36
TOl

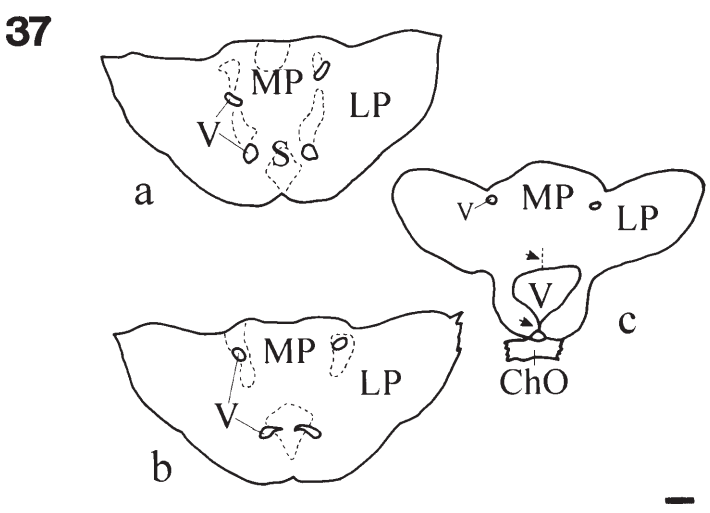
37
MP
LP
V
S
a
V
MP
LP
V
c
ChO
MP
LP
V
b

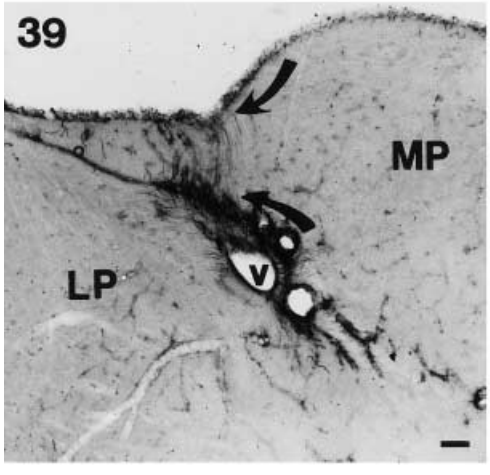
39
MP
LP
V

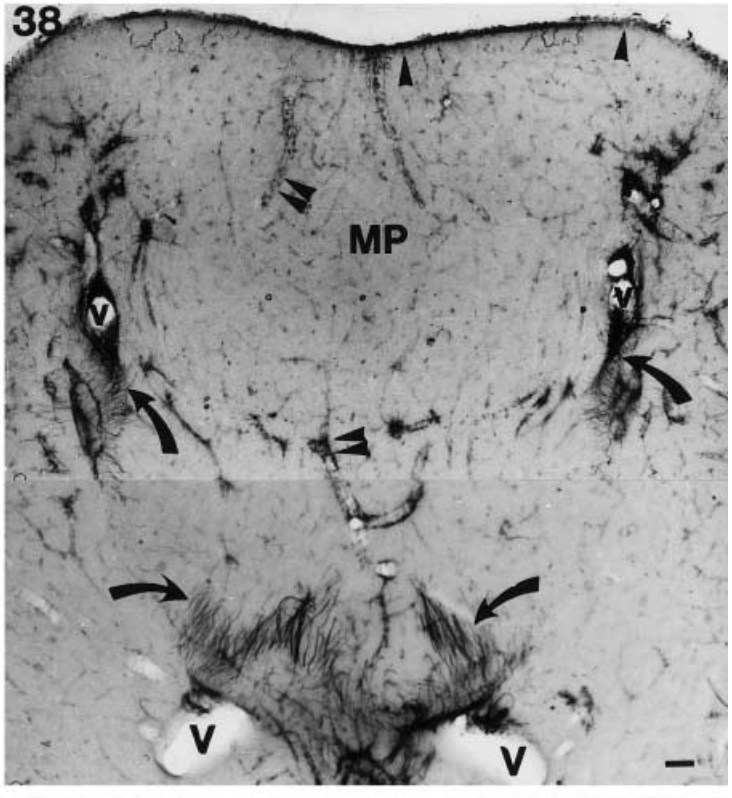
38
MP
V
V
V
V


41

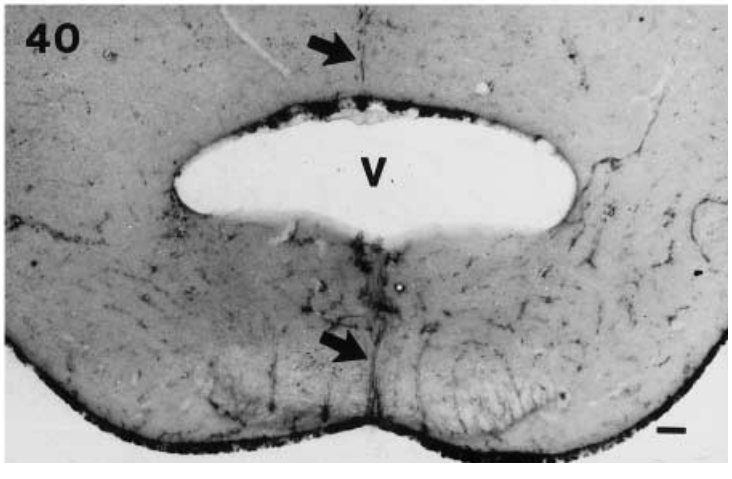
40
V

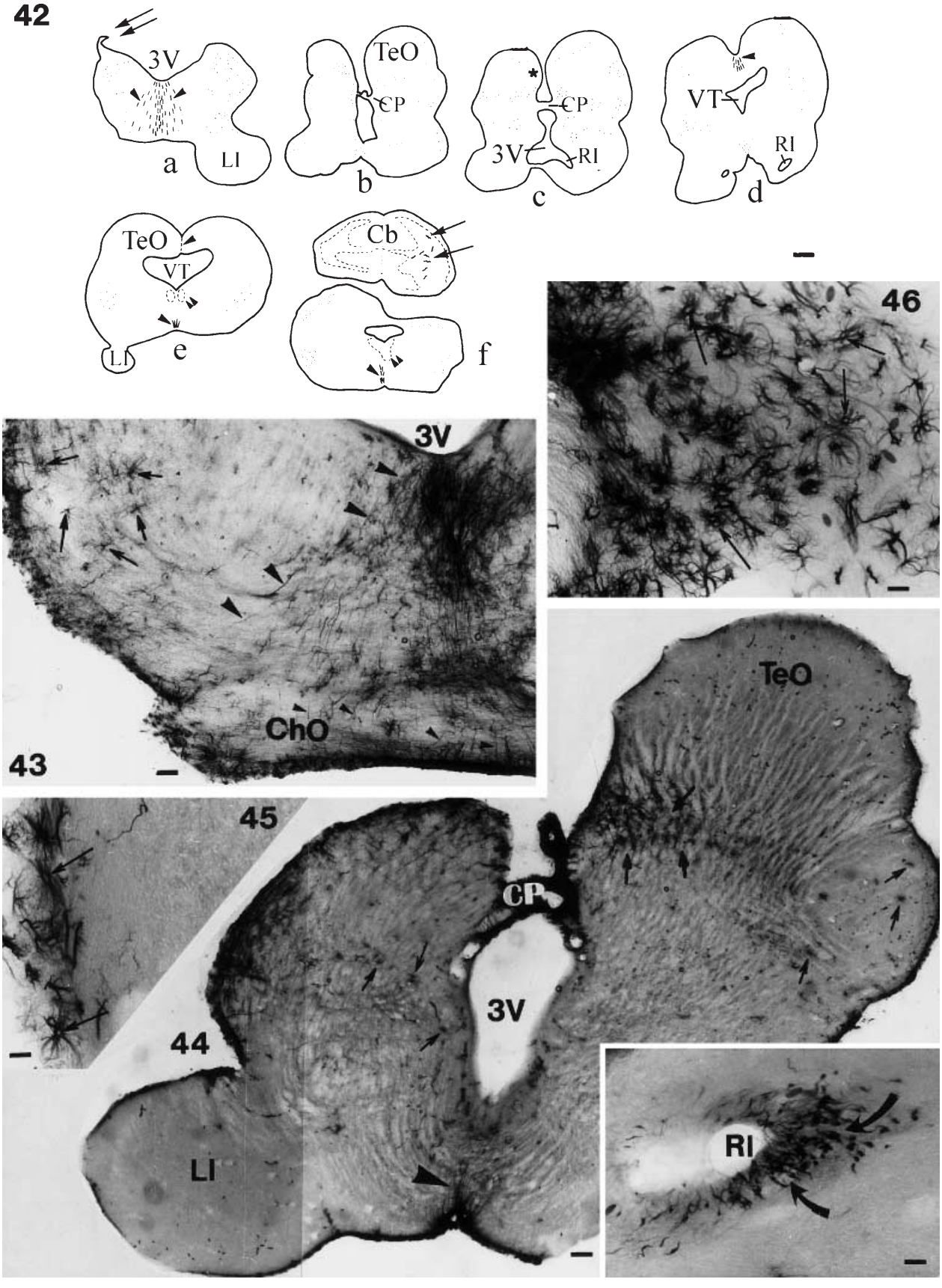
42
3V
LI
a
TeO
CP
b
CP
3V
RI
c
VT
RI
d
TeO
VT
LI
e
Cb
f
46
3V
ChO
43
TeO
45
CP
3V
44
LI
RI

forms between fiber-like and astrocyte-like glial elements are also visible (see also Fig. 54). It seems to be noteworthy that astrocytes and radial glia fibers frequently intermingle, e.g., in the middle of the diencephalon, (Fig. 50), in the optic chiasm, (Fig. 47) and in the posterior commissure (Fig. 49).

Raia erinacea: rhombencephalon and cerebellum

Our description follows a caudo-rostral direction. The contours of the cross-sections, with a part of the cerebellum, are shown in Fig. 60. In the "closed" part of the rhombencephalon, caudal to the ventricle (Fig. 61) only the midline septum and large glial septa between the brain tracts (e.g., medial longitudinal fasciculus) are intensely immunopositive. In more rostral sections, only the grey matter in the corner of the ventricle contains intensely GFAP-immunostained fibers (Fig. 62). In the surrounding areas, a faint "reticular" glial pattern, resembling that seen in *Squalus* (Figs. 19–23) is apparent. Throughout the medial part of the rhombencephalon, GFAP-immunopositive fibers are most prominent in the midline and in thick septa that separate brain tracts (Fig. 63). In the intracerebral parts of cranial nerves a number of GFAP-immunopositive fibers are parallel with the nerve fibers. Other glial fibers form septa between the bundles of nerve fibers (Fig. 64). A few astrocytes are also detected here. Otherwise, however, no GFAP-immunopositive astrocytes are present in the rhombencephalon, in contrast to the more rostral brain parts.

The cross-section of the *Raia* cerebellum indicates a foliated structure. Actually, in skates sulci divide the cerebellum into numerous folium-like sublobuli. These convolutions, however, involve the entire cerebellar wall including its ventricular surface, whereas in mammals and birds only the outer wall surface forms the folia (Nieuwenhuys 1967). Only very few GFAP-immunopositive elements are present in the *Raia* cerebellum: a few huge astrocytes are noteworthy in the white matter, proving the effect of the staining (Fig. 65).

Discussion

As shown previously, both shark and skate astroglia can be immunostained with mammalian anti-GFAP immunglobulin (*Squalus acanthias*: Dahl and Bignami 1973; Gould et al. 1995; *Mustelus canis*, *Raia ocellata*: Dahl et al. 1985). Our study extends the previous works, as it is the first to map systematically and compare GFAP-immunopositive structures in whole chondrichthyan brains. Despite the phylogenetical relationship between *Squalus acanthias* and *Raia erinacea* (Smeets et al. 1983), there were striking differences in their astroglia. On the basis of our GFAP study, the systematic differences are two:

1. In *Raia* radial glia were confined to a few areas, and astrocytes occurred in every main brain area. In *Squalus* radial glia were ubiquitous, predominant structures, whereas astrocytes were not seen.
2. In *Raia* most brain regions had only few GFAP-immunopositive structures, whereas in *Squalus* GFAP immunopositivity was almost evenly distributed, except in the gray and white matters of the spinal cord and brain stem, and the granular and molecular layers of the cerebellum.

In *Squalus*, GFAP staining distinguished layers in both the telencephalon and the tectum as well as in molecular and granular layers of the cerebellum. The meningeal surface was lined by radial glial endfeet. Perivascular glia were composed from a combination of endfeet, enpassing contacts and thin fiber plexuses.

In *Raia* telencephalic, tectal and cerebellar layers were not distinguished with GFAP immunostaining. The meningeal and perivascular glia were composed mainly of astrocytes. Radial ependymoglia were found in only a few parts of the ventricular system. Only where the ventricular system approached the meningeal surface (dorsal recess of the telencephalic ventricle, midpart of the dien-

◀ **Fig. 42** Schematic drawings of the cross-sections with *Raia* diencephalon and mesencephalon, in rostro-caudal order (**a–f**). (*CP* posterior commissure, *LI* lobus inferior of hypothalamus, *RI* inferior recess of the third ventricle in the inferior lobe of hypothalamus, *TeO* optic tectum, *3V* third ventricle, *VT* tectal ventricle). *Arrowheads* point to the dorsal and ventral midline glial septa (see enlarged in Figs 43, 52 and 53), *double arrowheads* point to the medial longitudinal fascicle, *double arrow* points to the torn edge of the roof of the third ventricle (the lamina epithelialis). The scattered points mark the positions of large astrocytes (see enlarged in Figs 55 to 59). *Asterisk* indicates the area shown in Fig. 54. A part of the cerebellum (*Cb*) already appears, the dotted line symbolizes the border of the cerebellar cortex, *arrows* point to large astrocytes, for their photomicrograph see Fig. 63. *Bar* 1 mm

Fig. 43 Cross-section of the *Raia* diencephalon, at the optic chiasm, just rostrally from Fig. 42a. In the middle, a strongly stained radial fiber system (*arrowheads*) fans out from the third ventricle (*3V*) toward the basal surface. It penetrates (*small arrowheads*) the optic chiasm (*ChO*). The fiber system is denser in the middle. In the lateral part of the diencephalon there are no long fibers, only astrocytes (*arrows*). *Bar* 200 µm

Fig. 44 Cross-section at the border of the diencephalon and mesencephalon of *Raia*, near Fig. 42c. Note the thick walls and that large parts of the cross-section are poor in GFAP. *Arrows* indicate GFAP-immunopositive astrocytes. (*CP* posterior commissure, *LI* inferior lobe of hypothalamus, *TeO* tectum, *3V* third ventricle). *Arrowhead* points to the ventral glial septum, a rest of the radial fiber system shown in Fig. 43. Enlarged inset (lower right corner) displays GFAP-immunopositive ependymal cells (*curved arrows*) around the inferior recess (*RI*) of the third ventricle in the inferior lobe of hypothalamus. *Bar* 300 µm; *inset bar* 30 µm

Fig. 45 Astrocytes on the meningeal surface of the *Raia* mesencephalon. Similar limiting glia are present on other *Raia* brain surfaces. Note that astrocytes are spread along the surface. This position is easy to study in the next Fig. 46. *Arrows* point to the GFAP-free places of nuclei. *Bar* 60 µm

Fig. 46 Tangential section to the surface. Note that astrocytes are spread along the surface and form a dense meshwork of processes. *Arrows* point to the GFAP-free places of nuclei. *Bar* 60 µm


47

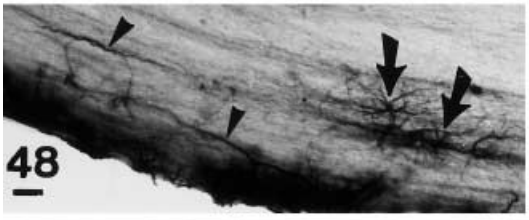
48

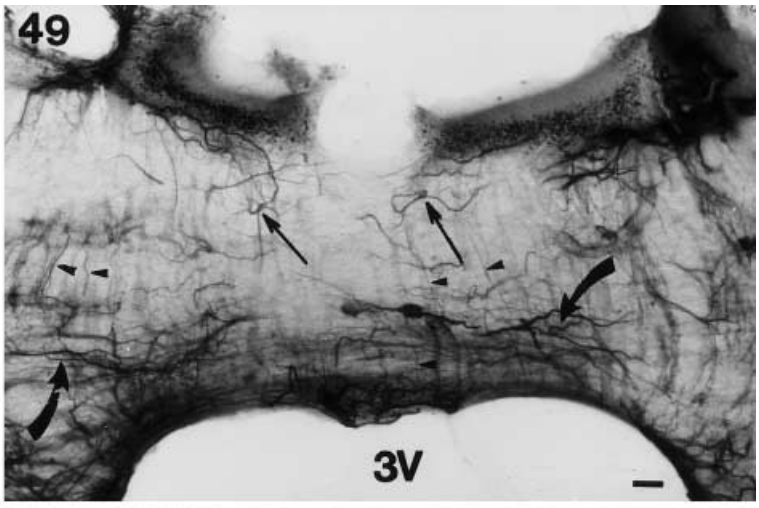
49
3V


50

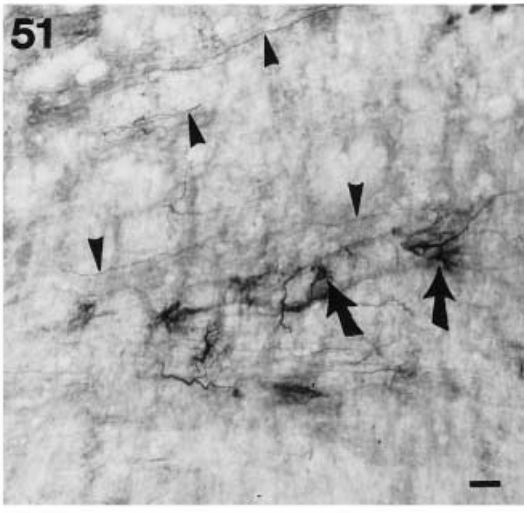
51


52

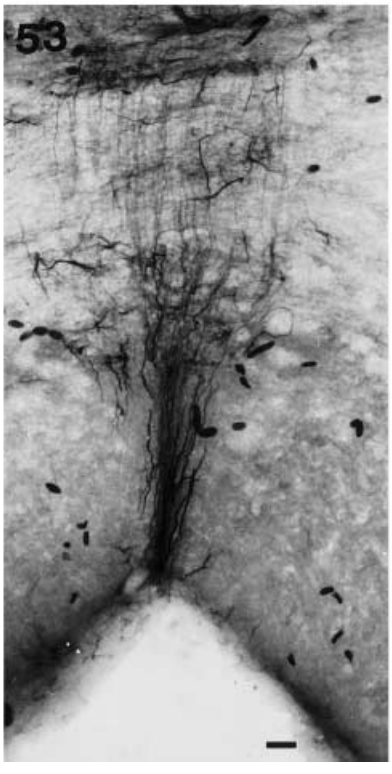
53


54

cephalon, mesencephalic dorsal and ventral raphe) could radial fibers be followed from surface to surface. It is to be emphasized, however, that according to our results *Raia* brain does contain radial fibers in several part of the brain, only these fibers do not form a ubiquitous and predominating system, and are frequently intermingled with astrocytes. It seems likely that the periventricular radial fibers, the fine, short fiber segments in the lateral pallium (or in the mesencephalic tegmentum, respectively), and the fibers that end at the meningeal surface are components of the same glial system, only their continuity is not obvious in sections.

Whereas glial structures were very different in the prosencephalon and mesencephalon of the two species, in the rhombencephalon they were quite similar, except in the cerebellum. In both species, GFAP-immunopositive elements took on a "reticulated" composition, corresponding to the formatio reticularis. The strongly-stained midline glial septa and lesser glial septa that separate nerve fiber bundles were also common to both species.

Our observations of the ependymoglial system of the *Squalus* brain generally agreed with observations using Cajal impregnation methods in *Scyliorhinus canicula* (Horstmann 1954). However, by immunostaining against GFAP we did not detect any astrocytes in the spiny dogfish brain. Smeets and Nieuwenhuys (1976) found predominantly radial glia in *Squalus acanthias* and (the galeomorph) *Scyliorhinus canicula* brain stem applying impregnation techniques. Roots (1986) also concluded, from a review of data that used impregnation and electron microscopic methods, that shark brains contained mainly ependymoglia. On *Ginglymostoma ciriratum* ependymoglia (tanycytes) were reported by Schroeder and Ebbesson (1975). The reports on astrocytes in sharks are associated to galeomorph sharks (Horstmann 1954, *Scyliorhinus canicula*; Long et al. 1968, by Cajal impregnation and electron microscopy, *Sphyrna zygaena*, *Galeocerdo cuvieri* and *Ginglymostoma ciriratum*). These astrocytes were mainly concentrated around vessels and along the meningeal surface, like those found by us in *Raia***.** Immunostaining of S-100 protein detected radial fibers, perivascular fibers and Bergmann glia in the galeomorph sharks *Scyliorhinus torazame* and *Mustelus manazo*, as well as a few astrocyte-perikaryon-like structures (Chiba 2000).

Horstmann (1954) observed astrocytes in *Torpedo marmorata* and *Raia radiata* brains. However, he only showed a single highly magnified area. Gotow and Hashimoto (1984) identified astrocytes in a sting ray (*Dasyatus akajei*), by electron microscopy. The preferred locations of astrocytes in *Raia* were around blood vessels and at the meningeal surface. These locations are in accord with the fact that perivascular glia form the blood-brain barrier in chondrichthyans (Bundgaard and Cserr 1981, 1991; Gotow and Hashimoto 1984). According to Achucarro (1915), perivascular glia appear first independently from ependymoglia in vertebrates.

Like chondrichthyans, teleost fishes also have high amounts of ependymoglia. These are rather evenly distributed (except for a few confined areas, e.g., in the vagal and facial lobes). Teleosts also lack GFAP-immunopositive astrocytes (Kálmán 1998). Although the *Squalus* glia resembled, more or less, that of bony fishes, neither *Raia,* nor *Squalus* brain contained thick, extended ependymoglial plexuses characteristic of teleost brains (e.g., carp, *Cyprinus carpio*, Kálmán 1998) in the tectal and rhombencephalic ventricles. In carp brain many glial fibers are oriented parallel with nerve fibers. In *Squalus* and *Raia* brains they are found only in a few areas, as the optic chiasm, posterior commissure, olfactory tract, and the emergence of cranial nerves. In *Squalus* the perivascular glial consisted of plexuses of fine fibers as well as endfeet and en passant connections of radial glia. Unlike carp (Kálmán 1998), glial fibers do not appear to attach along the vessels.

From our experience with astroglia in different amniotes (Hajós and Kálmán 1989; Kálmán and Hajós 1989; Kálmán et al. 1993, 1994), it seemed that differences between *Squalus* and *Raia* were much like differences between reptiles and mammals plus birds. Despite their different origins (synapsid and diapsid, respectively), mammals and birds have similar astroglia. In both groups astrocytes predominate and the GFAP immunopositivity is unevenly distributed, i.e., large brain areas are mostly devoid of it, despite the intense immunopositivity of adjacent areas (e.g., neostriatum and paleostriatum augmentatum in chicken, and the middle zone of

◀ **Fig. 47** Detail of the optic chiasm of *Raia*, penetrated by GFAP-immunopositive fibers (*small arrowheads*), and astrocytes (*arrows*). *Bar* 40 μm

Fig. 48 Detail of the optic tract of *Raia*. Here astrocytes (*arrows*) are scarce but extra large. A few glial fibers (*arrowheads*) are directed along the optic fibers. *Bar* 100 μm

Fig. 49 Posterior commissure of *Raia*. *Arrowheads* point to perpendicular (i.e., radial) fibers. Another, strongly stained population (*curved arrows*) runs transversally (i.e., along the nerve fibers). Astrocyte-like forms (*arrows*) are also seen (*3V* third ventricle). *Bar* 60 μm

Fig. 50 Radial glial fibers (*arrowheads*) in the medial part of the *Raia* diencephalon, intermingled with astrocytes (*arrows*). *Bar* 60 μm

Fig. 51 GFAP-poor area in the lateral region of the tegmentum of the *Raia* mesencephalon. Only a few fibers (*arrowheads*) are seen oriented toward the meningeal surface. The perivascular astrocytes (*arrows*) less densely colonize the vessels than in the telencephalon. *Bar* 60 μm

Fig. 52 Thick bundle of radial fibers in the dorsal midline glial septum of the *Raia* mesencephalon, between the two halves of the optic tectum. *Bar* 60 μm

Fig. 53 Radial fibers in the ventral midline glial septum of the *Raia* mesencephalon, through the tegmentum from the bottom of the ventricle. *Bar* 150 μm

Fig. 54 Long glial fibers form endfeet (*small curved arrows*) on the medial side of the optic tectum of *Raia*, immediately above the posterior commissure (for anatomical position, see asterisk in Fig. 41c). Their origin could not be traced. *Arrows* point to intermediate forms between fiber-like and astrocyte-like glial elements. *Bar* 60 μm

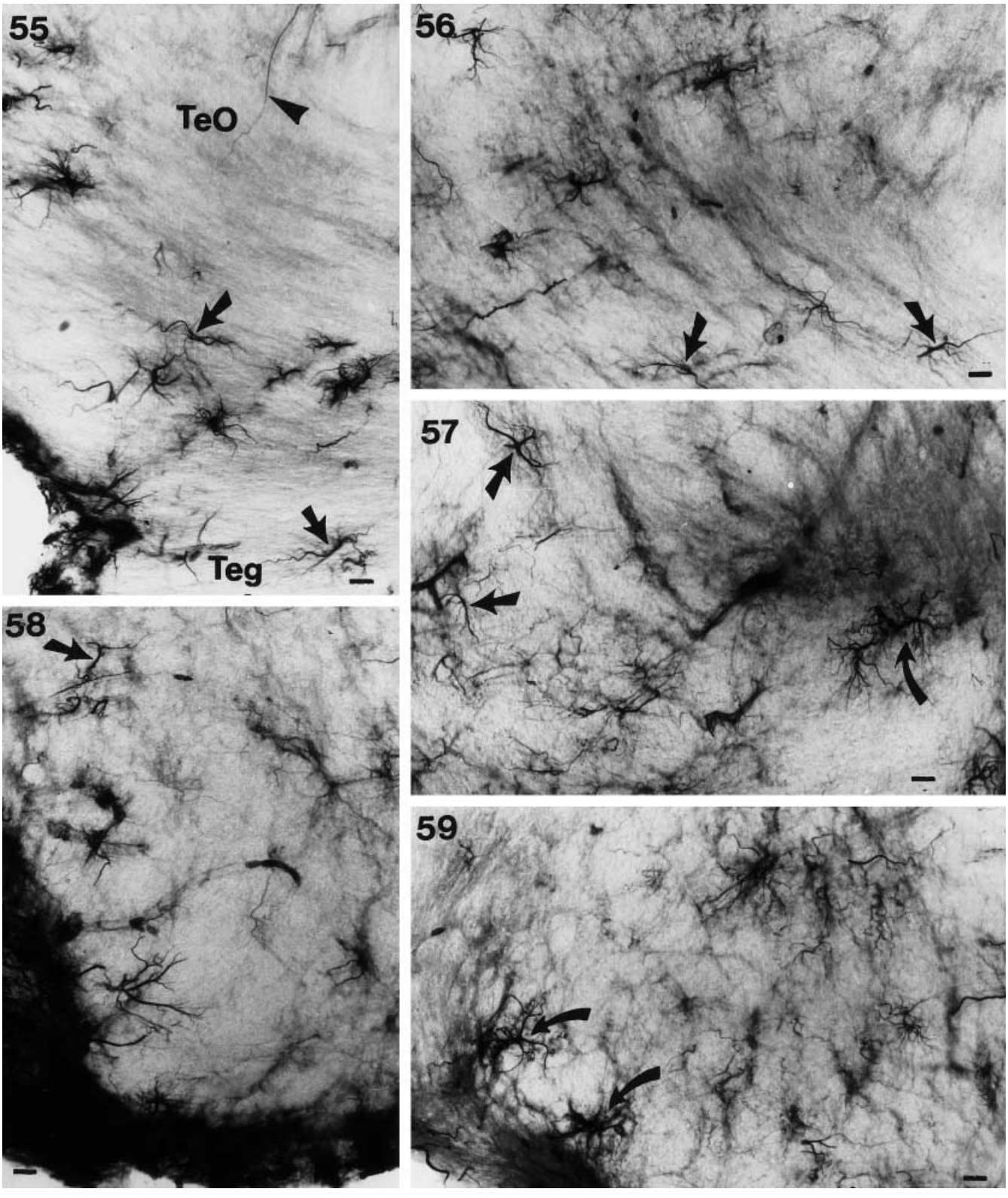

Figs. 55–59 Astrocytes of *Raia* diencephalon and mesencephalon (see points in Fig. 42). *Arrows* point to forms with few processes, as if intermediate forms between fiber-like and astrocyte-like glial elements. *Curved arrows* point to extra large forms. *Arrowhead* indicates a long fiber. *Bars* 60 µm

Fig. 55 At the joint of the optic tectum (*TeO*) and tegmentum (*Teg*)

Fig. 56 In the ventral part of the tectum

Fig. 57 In the dorsal part of the mesencephalic tegmentum

Fig. 58 In the basolateral part of the diencephalon

Fig. 59 In the basal part of the mesencephalic tegmentum

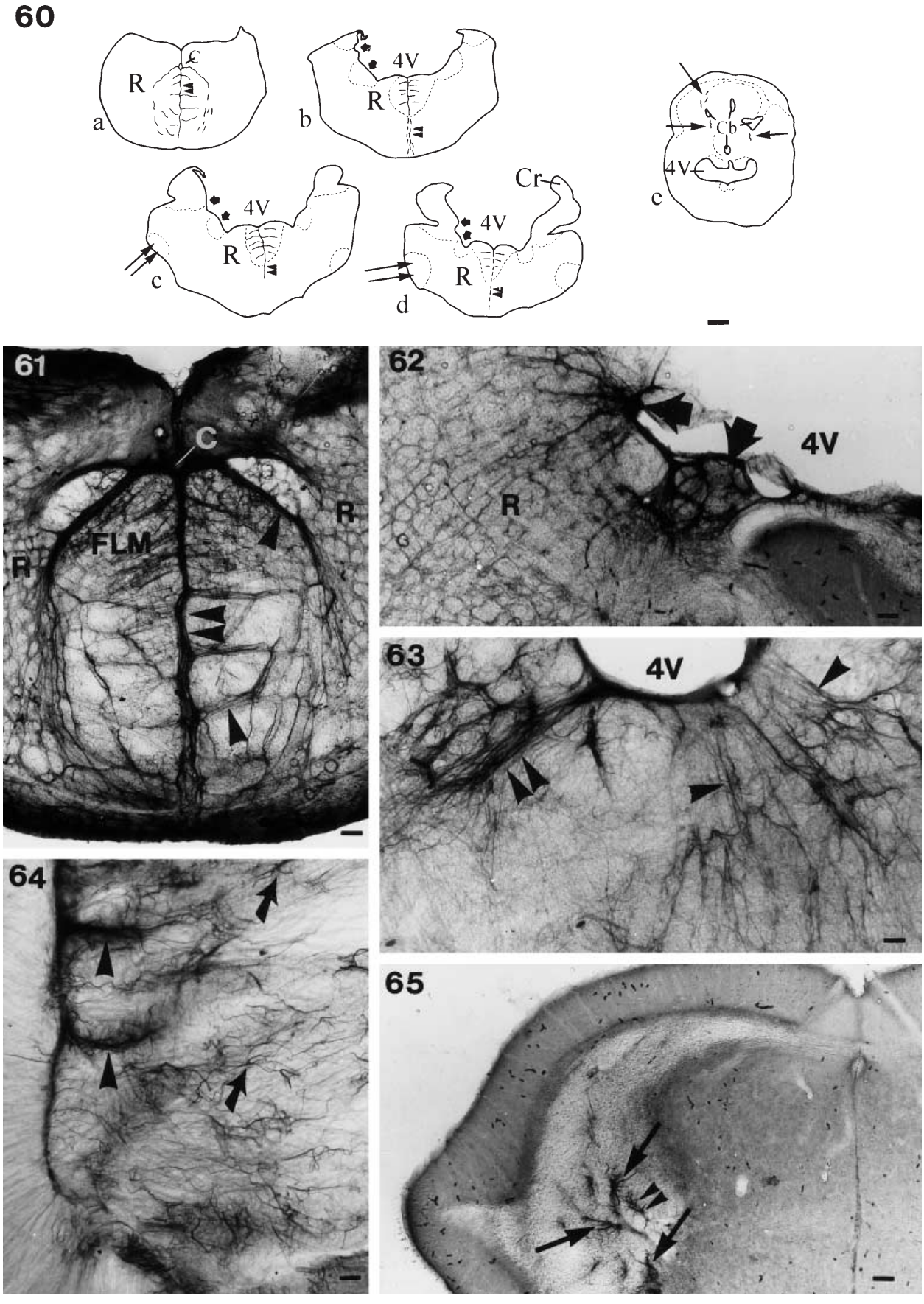

Fig. 60–65 Legends see page 78

cortex, striatum, colliculi superior and inferior in rat, Ludwin et al. 1976; Hajós and Kálmán 1989; Kálmán and Hajós 1989; Zilles et al. 1991; Kálmán et al. 1993). Uneven GFAP distribution was also seen in biochemical studies (Patel et al. 1985). In reptilian brains, radial glia predominate and the GFAP distribution is relatively uniform (Monzon-Mayor et al. 1990; Yanes et al. 1990; Kálmán et al. 1994). As in *Raia*, the Bergmann glia in birds lack GFAP (Dahl et al. 1985; Roeling and Feirabend 1988; Kálmán et al. 1993).

One should realize that lack of GFAP immunopositivity does not mean lack of astroglia. Astroglia can be present without expressing detectable GFAP (Connor and Berkowitz 1985; Linser 1985). An intense GFAP immunopositivity appears when areas that are nearly devoid of GFAP in intact mammals or birds are injured (Bignami and Dahl 1976; Bignami et al. 1980; Székely et al. 1991; Ajtai and Kálmán 1998). These results indicate that "GFAP-free" astrocytes have a capability of stimulus-induced GFAP expression (reviewed Hajós and Zilles 1995). Similar phenomena may be expected in skates as well.

A common feature, which distinguishes brains of mammals, birds and skates from those of reptiles and the squalomorph sharks, is the brain-wall thickness, reflecting the complexity of brain. Skates have narrow, slit-like telencephalic and mesencephalic ventricles and thick walls, in contrast to the squalomorph sharks. Note that the rhombencephalons of sharks and skates have similar anatomy and also similar glial structure.

It has been suggested by several authors that the replacement of radial glia with astrocytes is related to the thickening of the brain wall both in ontogenesis (Hajós and Bascó 1984) and in phylogenesis (Horstmann 1954; Naujoks-Mantauffel and Roth 1989; Wicht et al. 1994), during which brain-wall thickness might have determined the ratio of astrocytes to radial glia. This correlation is thought to be result of metabolic and homeostatic constraints (Oksche 1958; Reichenbach 1989). According to Reichenbach and colleagues (Eberhard and Reichenbach 1987; Reichenbach et al. 1987; Reichenbach 1989) the extreme elongation is disadvantageous for the radial glial fibers, because they are no longer capable of maintaining normal potassium equilibrium, and, therefore, they are stimulated to divide and transform into stellate cells. According to Mugnaini (1986) "a division of labor may be required by a thickened brain wall, especially in warm-blooded animals with high aerobic metabolism, resulting in separation of parietal functions (ependyma) and intrinsic or centralized functions (astrocytes)".

There are, however, meaningful features of the *Raia* astroglia that contradict this hypothesis. In *Raia*, radial fibers persist in several parts of the brain, although they do not predominate. There is no territorial distinction between the distribution of astrocytes and radial fibers, which frequently intermingle each other, and their distribution does not correlate strictly with the local thickness of the brain wall. Thus, in *Raia*, the appearance of astrocytes is probably not due only to the disappearance of radial fibers from the thickening brain walls. A relatively small ventricular surface compared with the meningeal surface may favor stellate cells, to complete the fiber system, which is dense at its ventricular origin, but becomes loose going to the meningeal surface. The persistence of radial fibers may also be attributed to a persistent neuron formation and migration in chondrichthyans. A similar phenomenon underlies the persistence of some radial fibers in birds, at the "hot spots" of the adult neuron formation (Alvarez-Buylla et al. 1987; 1990).

A further difference from mammals and birds is the extra large astrocytes in *Raia* (Figs. 47, 55–59, and also under low-power, Figs. 43, 44, 65). The arborization of *Raia* astrocytes is frequently simple (Figs. 47–49, 54–59), so several cells seem to represent intermediate forms with the radial glia. The GFAP-free places of nuclei are frequently visible (Figs. 33, 44). The perivascular and submeningeal astrocytes of *Raia* are spread along the surface, whereas in mammals the perikarya lie distant from the surface and send processes to it.

According to the classification of brain complexity by Butler and Hodos (1996), *Squalus* has a laminar brain ("type I"), while the *Raia* brain is of the elaborated type ("type II"). In accordance with this difference, Wicht et al. (1994) demonstrated GFAP-immunopositive astrocyte-like cells in the pacific hagfish (*Eptatretus stouti*,

◀ **Fig. 60** Schematic drawings of the cross-sections of the *Raia* rhombencephalon, with a part of the cerebellum, in caudo-rostral order (**a–e**, the latter is caudal to Fig. 42f; *C* central canal, *Cb* cerebellum, the pointers indicate parts of the narrow ventricular system, *Cr* cerebellar crest, *R* area of reticulated glial composition, *4V* fourth ventricle, *double arrowheads* point to the midline glial septum – see enlarged in Figs. 61 and 63, *double arrows* point to emergences of cranial nerves – see enlarged in Fig. 64, *arrows* point to large astrocytes in the cerebellum – see enlarged in Fig. 65, *small thick arrows* point to the grey matter). *Bar* 1 mm

Fig. 61 The middle zone of the "closed" part of the *Raia* rhombencephalon (see Fig. 60a). Only the midline glial septum (*double arrowhead*) and and its branches (*arrowheads*) between the neural tracts. Medial longitudinal fasciculus (*FLM*) are intensely immunopositive. A reticular glial pattern (*R*) that resemble the situation in *Squalus* is visible faintly (*C* central canal). *Bar* 300 µm

Fig. 62 Lateral corner of the fourth ventricle (*4V*) in *Raia* (for anatomical position see small thick arrows in Fig. 60). Only a confined area of grey matter (*thick arrows*) contains intensely GFAP-immunostained fibers. The surrounding area contains only faint contours of a reticular glial pattern (*R*). *Bar* 300 µm

Fig. 63 The medial part of the "open" *Raia* rhombencephalon (*4V* fourth ventricle). GFAP-immunopositive fibers occur only in the midline (*double arrowhead*), and separating the nerve fiber bundles (*arrowheads*). *Bar* 60 µm

Fig. 64 Emergence of a cranial nerve in *Raia*. For anatomical position, see double arrow in Fig. 60d. The GFAP-immunopositive fibers are parallel with the nerve fibers, which are bundled by thick glial septa (*arrowheads*). *Arrows* point to astrocyte-like forms. *Bar* 60 µm

Fig. 65 GFAP-immunopositive structures in the *Raia* cerebellum are represented only by a few large free astrocytes (*large arrows*) and perivascular astrocytes (*double arrowhead*). The cortex does not contain GFAP-immunopositive elements. *Bar* 150 µm

Myxiniformes), which represents an elaborated brain among agnathans. It should be noted, however, that every amniote brain is considered to be of type II, in spite of the above mentioned differences among mammals, birds and reptiles. Similarly, the teleosts, also with of type II brain, have mainly ependymoglia and only very few astrocytes (reviewed Kálmán 1998). The presence of the astrocytes, and even less their predominance, therefore, does not correlate strictly with the "elaborated" organization of the brain in every vertebrate group.

These results suggest that astrocytes appear and become predominant independently in different vertebrate stocks. The evolution of the astroglia also decreased the extension of the GFAP immunopositivity. These phenomena seem to be correlated with each other, because the appearance of astrocytes promotes the adaptation of the GFAP-content to the various local requests, and therefore the unnecessary expression of GFAP is avoided. The astrocytes can form a versatile glial network, and can promote (without a close correlation in distribution) both the thickening of the brain wall and the formation of local differences of astroglia.

It should be noted however, that the macroscopical structure of the brain of galeomorph sharks is similar to that of skates rather than squalomorph sharks (Northcutt 1981; Butler and Hodos 1996). Further studies, therefore, are required to see how the findings may be applied to galeomorph sharks.

Acknowledgements The fixation and the sectioning was performed at the Marine Biological Laboratory (Woods Hole, Mass., USA). A portion of this research was supported by grant RG2944 from the National Multiple Sclerosis Society (RMG). We thank J. Kiss for the photographic work, and E. Nemcsics for the line drawings.

References

Achucarro N (1915) De l'évolution de la névroglie, et spécialement de ses relations avec 1'appareil vasculaire. Trab Lab Invest Biol (Madrid) 13:169–212

Ajtai BM, Kálmán M (1998) Glial fibrillary acidic protein expression but no glial demarcation followes the lesion in the molecular layer of cerebellum. Brain Res 802:285–288

Alvarez-Buylla A, Buskirk DR, Nottebohm F (1987) Monoclonal antibody reveals radial glia in adult avian brain. J Comp Neurol 264:159–170

Alvarez-Buylla A, Theelen M, Nottebohm F (1990) Proliferation "hot spots" in adult avian ventricular zone reveal radial cell division. Neuron 5: 101–109

Ariens-Kappers CU Huber CG, Crosby EC (1960) The comparative anatomy of the nervous system of vertebrates, including man. Hafner, New York

Bignami A, Dahl D (1976) The astroglial response to stabbing. Immunofluorescence studies with antibodies to astrocyte-specific protein (GFA) in mammalian and submammalian vertebrates. Neuropathol Appl Neurobiol 2:99–110

Bignami A, Dahl D, Rueger D.C. (1980) Glial fibrillary acidic protein (GFAP) in normal cells and in pathological conditions. Adv Cell Neurobiol 1:285–310

Bignami A, Perides G, Asher R, Dahl D (1992) The astrocyte-extracellular matrix complex in CNS myelinated tracts: a comparative study on the distribution of hyaluronate in rat, goldfish and lamprey. J Neurocytol, 21:604–613

Bodega G, Suarez I, Rubio M, Fernandez B (1990) Distribution and characteristics of the different astroglial cell types in the adult lizard (*Lacerta lepida*). Anat Embryol 181:567–575

Bullock TH, Moore JK, Fields RD (1984) Evolution of myelin sheats: both lamprey and hagfish lack myelin. Neurosci Lett 48:145–148

Bundgaard M, Cserr HF (1981) A glial blood-brain barrier in elasmobranchs. Brain Res 226:61–73

Bundgaard M, Cserr HF (1991) Barrier membranes at the outer surface of the brain of an elasmobranch, *Raia erinacea*. Cell Tissue Res 265:113–120

Butler AB, Hodos W (1996) Vertebrate neuroanatomy. Evolution and adaption. John Wiley, New York, Chichester, Brisbane

Chiba A (2000) S-100 protein-immunoreactive structures in the brains of the elasmobranchs *Scyliorhinus torazame* and *Mustelus manazo.* Neurosci Lett 279:65–68

Connor JR, Berkowitz RM (1985) A demonstration of glial filament distribution in astrocytes isolated from rat cerebral cortex. Neuroscience 16:33–44

Dahl D, Bignami A (1973) Immunohistochemical and immunofluorescence studies of the glial fibrillary acidic protein in vertebrates. Brain Res 61:279–283

Dahl D, Crosby CJ, Sethi A, Bignami A (1985) Glial fibrillary acidic (GFA) protein in vertebrates: immunofluorescence and immunoblotting study with monoclonal and polyclonal antibodies. J Comp Neurol 239:75–88

Eberhardt W, Reichenbach A (1987) Spatial buffering of potassium by retinal Müller (glial) cells of various morphologies calculated by a model. Neuroscience 36:121–144

Gotow T, Hashimoto PH (1984) Plasma membrane organization of astrocytes in elasmobranch with special reference to the brain barrier system. J Neurocytol 13:727–742

Gould RM, Fannon AM, Moorman SJ (1995) Neural cells from dogfish embryos express the same subtype-specific antigens as mammalian neural cells in vivo and in vitro. Glia, 15:401–418

Hajós, F, Bascó E (1984) The surface-contact glia. Adv Anat Embryol Cell Biol 84:1–81

Hajós F, Kálmán M (1989) Distribution of glial fibrillary acidic protein (GFAP)-immunoreactive astrocytes in the rat brain. II. Mesencephalon, rhombencephalon and spinal cord. Exp Brain Res 78:164–173

Hajós F, Zilles K (1995) Areas of "dormant" glial fibrillary acidic protein (GFAP) immunoreactivity in the rat brain as revealed by automated image analysis of serial coronal sections. Neurobiology 3:3–11

Houser GL (1901) The neurons and supporting elements of the brain of a selachian. J Comp Neurol 11:65–165

Horstmann E (1954) Die Faserglia des Selachegehirns. Z Zellforsch Mikrosk Anat 39:588–617

Kálmán (1998) Astroglial architecture of the carp (*Cyprinus carpio*) brain as revealed by immunohistochemical staining against glial fibrillary acidic protein (GFAP). Anat Embryol 198:409–433

Kálmán M, Hajós F (1989) Distribution of glial fibrillary acidic protein (GFAP)-immunoreactive astrocytes in the rat brain. I.Forebrain. Exp Brain Res 78:147–163

Kálmán M, Székely A, Csillag A (1993) Distribution of glial fibrillary acidic protein-immunopositive structures in the brain of the domestic chicken (*Gallus domesticus*). J Comp Neurol, 330:221–237

Kálmán M, Kiss Á, Majorossy K (1994) Distribution of glial fibrillary acidic protein-immunopositive structures in the brain of the red-eared freshwater turtle (*Pseudemys scripta elegans*). Anat Embryol, 189:421–434

Linser PJ (1985) Multiple marker analysis in the avian optic tectum reveals three classes of neuroglia and carbonic anhydrase-containing neurons. J Neurosci 5:2388–2396

Long DM, Bodenheimer TS, Hartmann JF, Klatzo J (1968) Ultrastructural features of the shark brain. Am J Anat, 122:209–236

Ludwin SK, Kosek JC, Eng LF (1976) The topographical distribution of S-100 and GFA proteins in the adult rat brain. An immunocytochemical study using horseradish peroxidase-labelled antibodies. J Comp Neurol 165:197–208

Martin AP, Naylor GJP, Palumbi SR (1992) rates of mitochondrial evolution DNA evolution in sharks are slow compared with mammals. Nature 357:153–155

Monzon-Mayor M, Yanes C, Tholey G, Barry J de, Gombos G (1990) Glial fibrillary acidic protein and vimentin immunohistochemistry in the developing and adult midbrain of the lizard *Gallotia galloti*. J Comp Neurol 295:569–579

Mugnaini, E (1986) Cell junctions of astrocytes, ependyma, and related cells in the mammalian central nervous system, with emphasis on the hypothesis of a generalized functional syncytium of supporting cells. In: Fedoroff S, Vernadakis A (eds) Astrocytes, vol 1. Academic Press, New York, pp 329–371

Naujoks-Manteuffel, C, Roth G (1989) Astroglial cells in a salamander brain (*Salamandra salamandra*) as compared to mammals: a glial fibrillary acidic protein immunohistochemistry study. Brain Res. 487:397–401

Nieuwenhuys R (1967) Comparative anatomy of the cerebellum. In: Fox CA, Snider RS (eds) Prog Brain Res, vol 25. Elsevier, Amsterdam, pp 1–93

Nieuwenhuys R, Ten Donkelaar HJ, Nicholson C (1997) The central nervous system of vertebrates, vol 2. Springer Berlin, Heidelberg, New York

Northcutt R (1978) Brain organization in the cartilaginous fishes. In: Hodgson ES, Mathewson RS (eds), Sensory biology of sharks, skates and rays, Arlington, Va., Office of Naval Research, pp. 117–193

Northcutt RG (1981) Evolution of the telencephalon in nonmammals. Annu Rev Neurosci 4:301–50

Oksche, A. (1958) Histologische Untersuchungen über die Bedeutung des Ependyms, der Glia und der Plexus chorioidei für den Kohlenhydratstoffwechsel des ZNS. Z Zellforsch Mikrosk Anat 48:44–129

Onteniente B, Kimura H, Maeda T (1983) Comparative study of the glial fibrillary acidic protein in vertebrates by PAP immunohistochemistry. J Comp Neurol 215:427–436

Patel AJ, Weir MD, Hunt A, Tahourdin CSM, Thomas DGT (1985) Distribution of glutamine synthetase and glial fibrillary acidic protein and correlation with glutamate decarboxylase in different regions of the rat central nervous system. Brain Res 331:1–10

Reichenbach A (1989) Glia:neuron index: review and hypothesis to account for different values in different mammals. Glia 2:71–77

Reichenbach, A., Neumann M, Brückner G (1987) Cell length to diameter relation of rat fetal radial glia – does impaired K+ transport capacity of long thin cells cause their perinatal transformation in multipolar astrocytes? Neurosci Lett 73:95–100

Roeling TAP, Feirabend HKP (1988) Glial fiber pattern in the developing chicken cerebellum: vimentin and glial fibrillary acidic protein (GFAP) immunostaining. Glia 1:398–402

Roots BI (1986) Phylogenetic development of astrocytes. In: Vernadakis A, Fedoroff S (eds) Astrocytes, vol. 1. Academic Press, New York pp 1–34

Schroeder DM, Ebbesson SOE (1975) Cytoarchitecture of the optic tectum in the nurse shark. J Comp Neurol, 160:443–462

Smeets WJA, Nieuwenhuys R (1976) Topographical analysis of the brain stem of the sharks *Squalus acanthias* and *Scyliorhinus canicula*. J Comp Neurol, 165:333–367

Smeets WJA, Nieuwenhuys R, Roberts BL (1983) The central nervous system of cartilaginous fishes, Springer Berlin, Heidelberg, New York, pp 1–256

Székely AD, Kálmán M, Csillag A (1991) Peroxidase-positive glia is present around stab wounds in chick but not in rat brain. Anat Anz [Suppl 1] 70:689–690

Wahneldt TV (1990) Phylogeny of myelin proteins. Ann NY Acad Sci, 605:15–28

Wahneldt TV, Matthieu J-M, Jeserich G (1986) Appearance of myelin proteins during vertebrate evolution. Neurochem Int 9:463–474

Wasowicz M, Pierre J, Reprant J, Ward R, Vesselkin NP, Versaux-Botteri C (1994) Immunoreactivity to glial fibrillary acidic protein (GFAP) in the brain and spinal cord of the lamprey (*Lampetra fluviatilis*) J Brain Res 1:71–78

Wicht H, Derouiche A, Korf, H-W (1994) An immunocytochemical investigation of glial morphology in the Pacific hagfish: radial and astrocyte-like glia have the same phylogenetic age. J Neurocytol 23:565–576

Yanes C, Monzon-Mayor M, Ghandour MS, Barry J de, Gombos G (1990) Radial glia and astrocytes in the adult and developing telencephalon of the lizard *Gallotia galloti* as revealed by immunohistochemistry with anti-GFAP and anti-vimentin antibodies. J Comp Neurol 295: 559–568

Zilles K, Hajós F, Kálmán M, Schleicher A (1991) Mapping of glial fibrillary acidic protein-immunoreactivity in the rat forebrain and mesencephalon by computerized image analysis. J Comp Neurol 308:340–355